Artificial structures in single crystalline lattices

Prasenjit Sen
School of Physical Sciences
Jawaharlal Nehru University
New Delhi - 110067

History

Nonequilibrium processing of silicon through MeV ion irradiation.

Energy loss mechanism – Coulomb explosion – Nonlinear processes.

Localization of vibrational energy following an ion irradiation process.

Entrapment at a desired location leading to silicon nanostructures with modified band-gaps.

Vibrational energy transport (nonlinear transport of energy) through linear chains of a single crystalline lattice.

An application.

NLDD05 Sevilla, March 3-4, 2005

History

1994 2212 oxide superconductor (c = 24Å) under 100 MeV ^{57}Fe irradiation turns to 2223 oxide superconductor (c = 30Å) at 80K.

Our interpretation : lattice excitation

1998 Online conductivity measurements under 200 MeV Ag irradiation produces conductivity jumps in pure nickel and iron, both on switch-on and switch-off of ion beam.

Our interpretation : dissipative structure formation

1999 The lineshapes of I-V response under irradiation completely analyzed, with particular emphasis on the long-time decay tail.

Our interpretation : decay, a product of shock waves

History

2000 - STM, AFM, micro-Raman and x-ray topography measurements confirm process of defect formation and defect removal under MeV ion irradiation.

Our interpretation : nonlinear transport of energy

Modification of a lattice by low energy keV ions

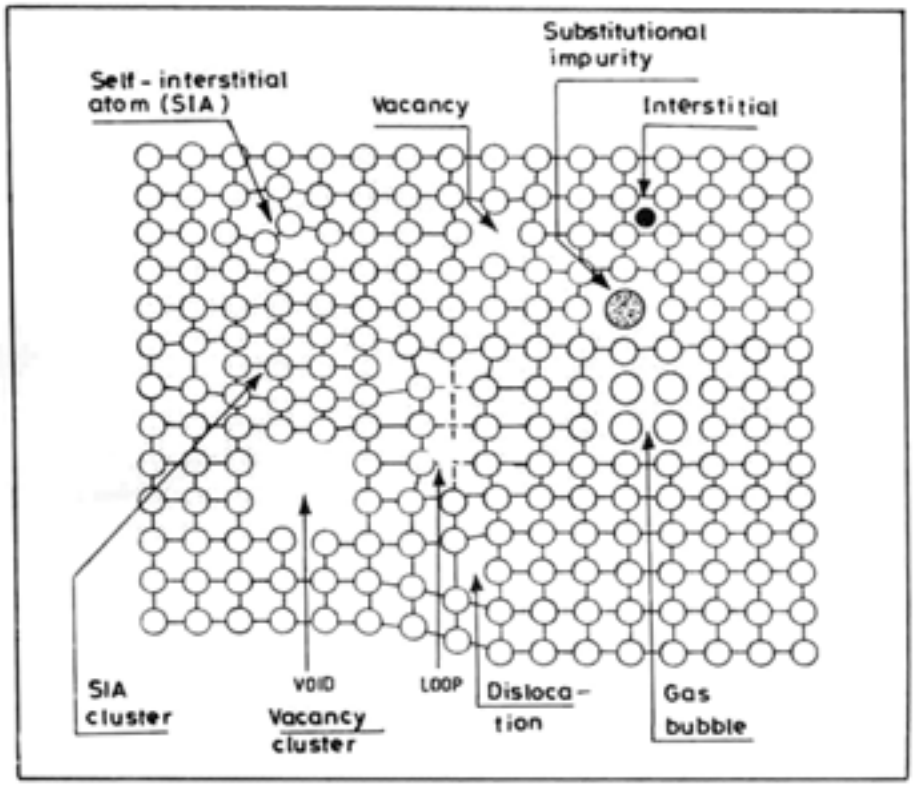

At keV energies, nuclear energy loss is predominant at the end of the ion range.

Result: Produces a rich variety of defects. Can be most suitably employed to perform substitution or doping for device manufacture.

Modification of a lattice by high energy MeV ions

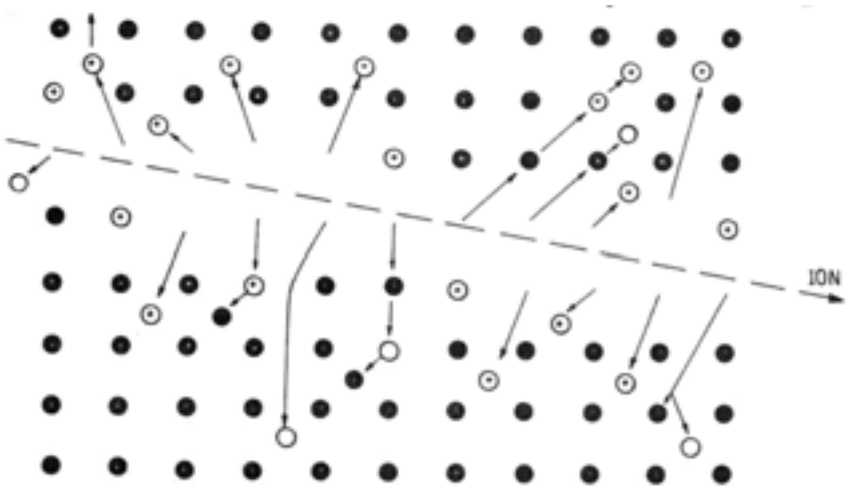

At MeV energies, electronic energy loss is predominant.

Result: In some cases (insulators and semiconductors) atoms can remain excited for a sufficiently long time and induce atomic movement through Coulomb repulsion.

Coulomb repulsion induces nonlinearity as it takes place in a time which is shorter than the inverse of the Debye frequency, ω_D (10^{-11} sec), for the lattice. This is similar to shock wave generation.

Nonlinearity can be naturally balanced by dispersion in the lattice to give localisation of vibrational energy.

The electronic energy loss of MeV ions

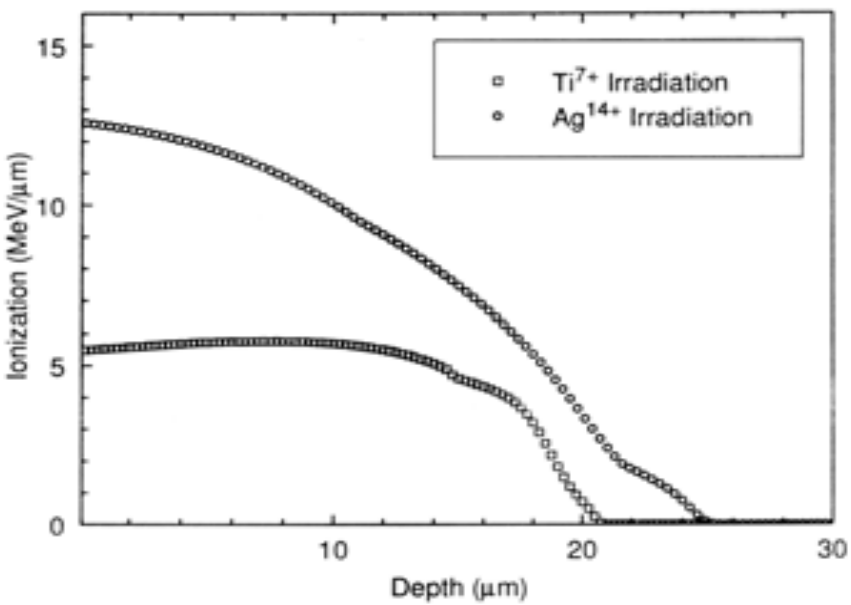

Electronic energy loss of 200 MeV Ag ions (*upper plot*) and 100 MeV Ti ions (*lower plot*) in silicon, employing TRIM.

The Ag ions continuously lose energy with depth travelled inside the sample. For Ti, the energy loss is almost constant till 0.75R.

MeV ions in silicon: The status in literature

Ref. No.	Authors	System	Inferences
1.	Levalois *et al.*, *NIM* B63, 14, 1992	3.6 GeV uranium ion in Si(100); S_e = 24 MeV/μm	TEM : No defects; Electronic energy loss ineffective
2.	Varichenco *et al.*, *NIM* B107, 268, 1996	5.68 GeV xenon ions in Si(111)	Amorphisation/disorder absent; suggests suppression of damage
3.	Furuno *et al.*, *NIM* B107, 223, 1996	Poly Si. Defects reported when S_e > 12 MeV/ μm	Track diameter scales with S_e
4.	Furuno *et al.*, *NIM* B107, 223, 1996	Poly Si, Ge and Ti	Susceptibility for S_e damage : Ti < Si < Ge

Inference : A material in single crystalline form with inherent long-range order is resistant to electronic energy loss, S_e or $(dE/dX)_e$.

Case of a line of atoms connected by harmonic springs

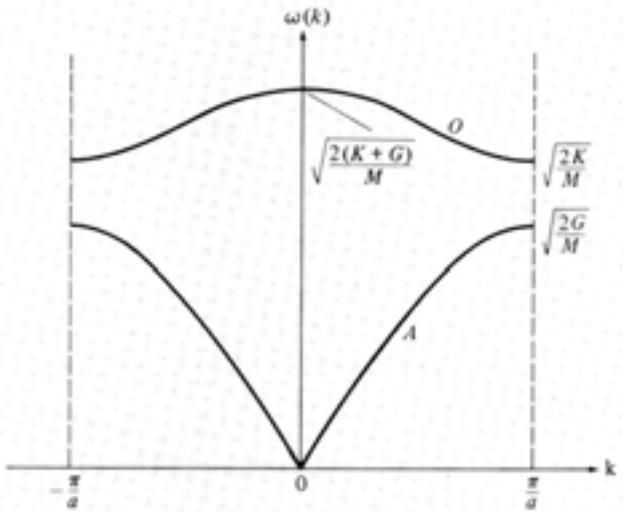

The primitive cell contains two ions joined by the K-spring, represented by the jagged line. In the acoustic mode, ions within cell move in phase while in the optic mode they move 180˚ out of phase.

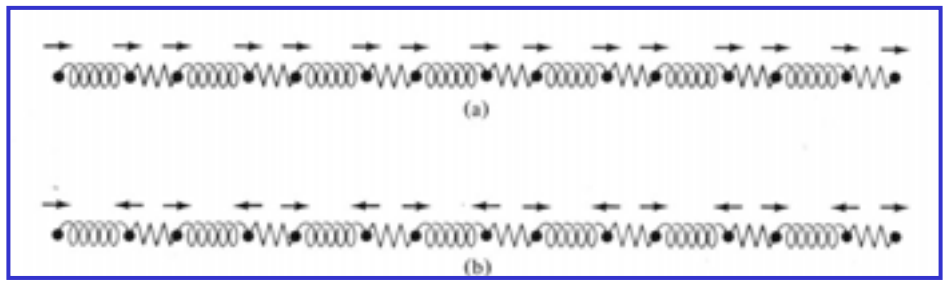

At k = 0 (centre of Brillouin zone)

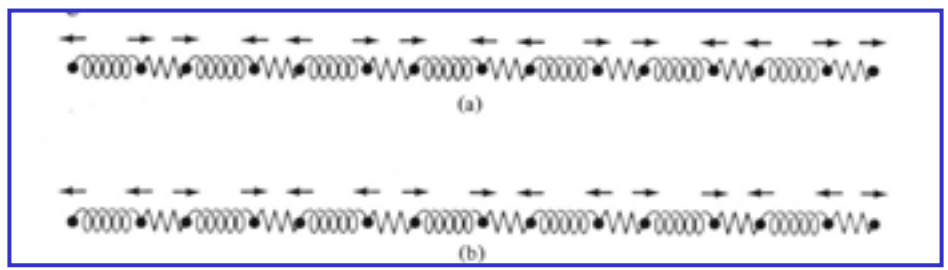

At k = ± π/a (edge of Brillouin zone)

$$U^{\text{harm}} = \frac{k_2}{2}\sum_n (u_{n+1} - u_n)^2,$$

Case of a line of atoms connected by anharmonic springs

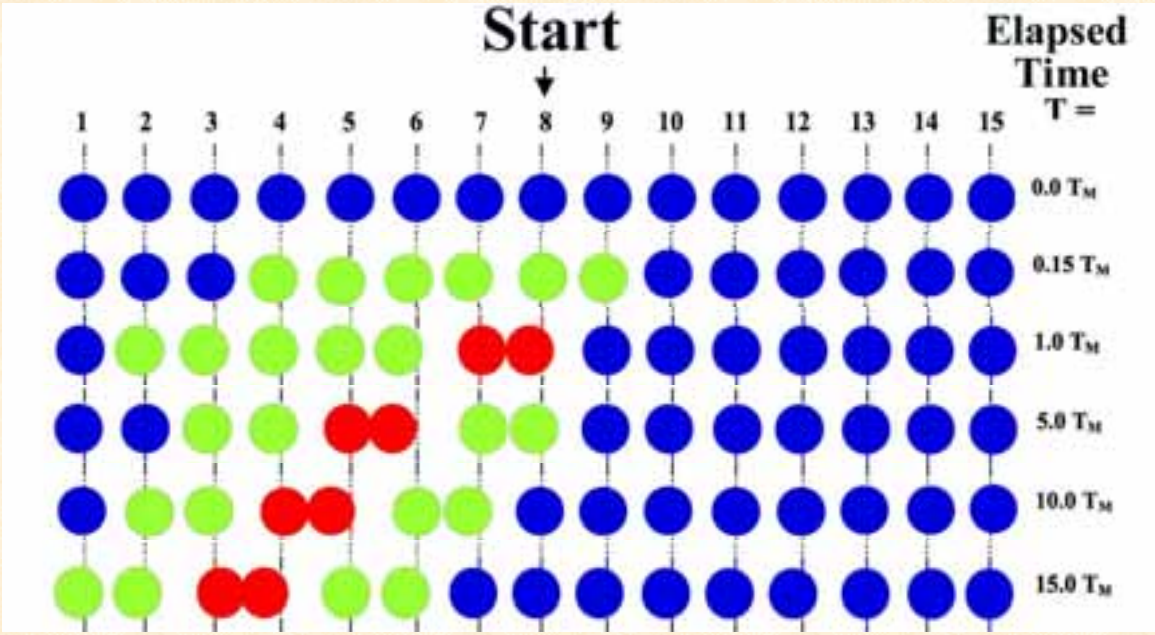

$$U^{\text{anharm}} = \frac{k_2}{2}\sum_n (u_{n+1}-u_n)^2 + \frac{k_4}{4}\sum_n (u_{n+1}-u_n)^4,$$

Dynamic evolution can be viewed at the website http://www.cornell.edu\sievers\ilm

Experiment to generate Irradiation Interfaces

Definition : Irradiation Interface is defined as the region between the irradiated and unirradiated sections of the sample.

Si(100)

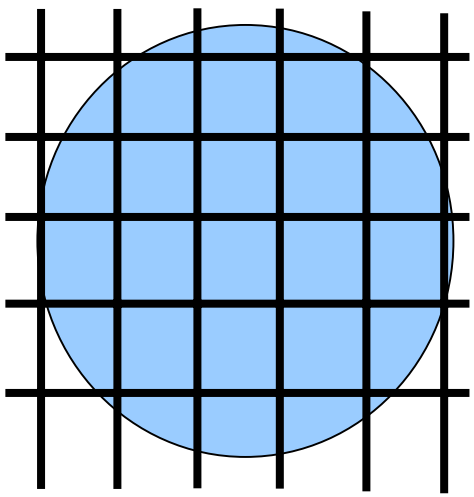

Ni wire, 40 μm square cross-section

Highlights :

X= 200 MeV Ag ion incident direction

Ni wire mesh held on top of Si(100) sample. Tested for mesh-sample distances of 5mm – 300 mm

200 MeV Ag ion range (R = 24 μm) in Si < 40 μm. Ions are stopped at the Ni mesh

Pelletron : schematic diagram

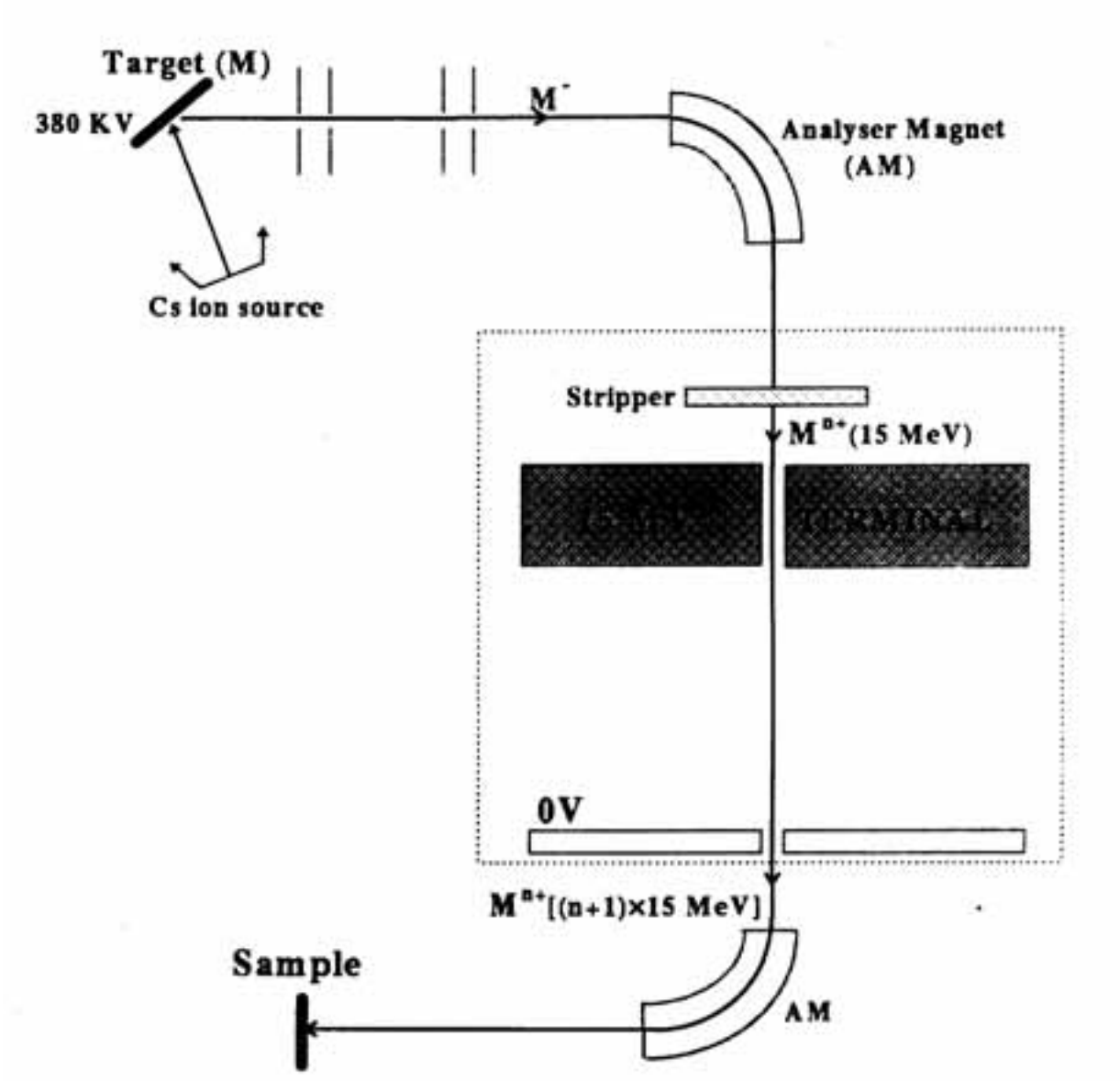

X-ray topography (XRT) results

I_{int} = integrated intensity, important in the experimental context. Experimental planes are large but finite. So, diffraction curve in not a delta function but has finite width, called Rocking Curve width. When angular divergence of the incident beam is >> RC width, we get total intensity from all planes within RC width(= Integrated Intensity)

$$I_{int} = I_e R^2 |F_g|^2 \frac{\lambda^3 \mathcal{V}}{\vartheta_a^2 \sin 2\theta}$$
$$= I_0 r_e^2 |F_g|^2 \left(\frac{\lambda^3 \mathcal{V}}{\vartheta_a^2 \sin 2\theta}\right) \overline{\mathcal{P}^2} \qquad (2.3)$$

where $I_e = I_0(r_e/R)^2 \overline{\mathcal{P}^2}$ ($r_e = 2.81 \times 10^{-13}$ cm, the classical Bohr radius) is the scattered intensity at a distance R by a single electron, I_0 is the intensity of the incident beam, $\mathcal{V}$ and ϑ_a are the crystal volume and unit cell volume respectively, F_g is the *structure factor* for the corresponding reflection and $\mathcal{P}$ is the *polarization factor*, defined as

$$\mathcal{P} = \begin{cases} \cos 2\theta & \text{for } \pi\text{-polarization} \\ 1 & \text{for } \sigma\text{-polarization} \end{cases} \qquad (2.4)$$

Integrated Intensity = max. intensity that can be diffracted by hkl planes

X-ray topography (XRT) results

t = path length traversed by x-rays in a crystal; ϕ = negative angle between the crystal surface and the diffracting planes. For a block lying at depth z from the surface, t is given by :

$$t = z\left(\frac{1}{\sin(\theta+\phi)} + \frac{1}{\sin(\theta-\phi)}\right)$$

Let A_0 be the cross sectional area of the incident beam. Then the area of the sample surface exposed to X-rays is $A_0/\sin(\theta-\phi)$. The number of diffracting blocks between depths z and $z+dz$ is $A_0 dz/\mathcal{V}\sin(\theta-\phi)$. Thus, the diffracted intensity from an imperfect crystal is given by

$$\begin{aligned} I_s &= I_{inf}\frac{A_0}{\mathcal{V}\sin(\theta-\phi)}\int_0^\infty e^{-\mu t}dz \\ &= P_0\, r_e^{\,2}\,|F_g|^2\left(\frac{\lambda^3}{\vartheta_a^{\,2}}\right)\left(\frac{1+\cos^2 2\theta}{2\sin 2\theta}\right)\left[\frac{1}{2\mu}(1+\cot\theta\,\tan\phi)\right] \end{aligned} \qquad (2.5)$$

where $P_0 = I_0 A_0$ is the incident power. Defining $\rho_s = I_s/I_0 A_0$, the integrated intensity per unit incident power is given by

$$\rho_s = r_e^{\,2}\,|F_g|^2\left(\frac{\lambda^3}{\vartheta_a^{\,2}\sin 2\theta}\right)\left[\frac{1}{2\mu}(1+\cot\theta\,\tan\phi)\right]\overline{\mathcal{P}^2} \qquad (2.6)$$

Integrated intensity given by Eq.(2.6) is one of the important expressions used in the interpretation of X-ray topographs, and is known as the *kinematic intensity*. In deriving this, we have considered the *secondary extinction* (extinction due to inelastic scattering) of the X-ray beam as it passes through the crystal.

X-ray topography (XRT) results

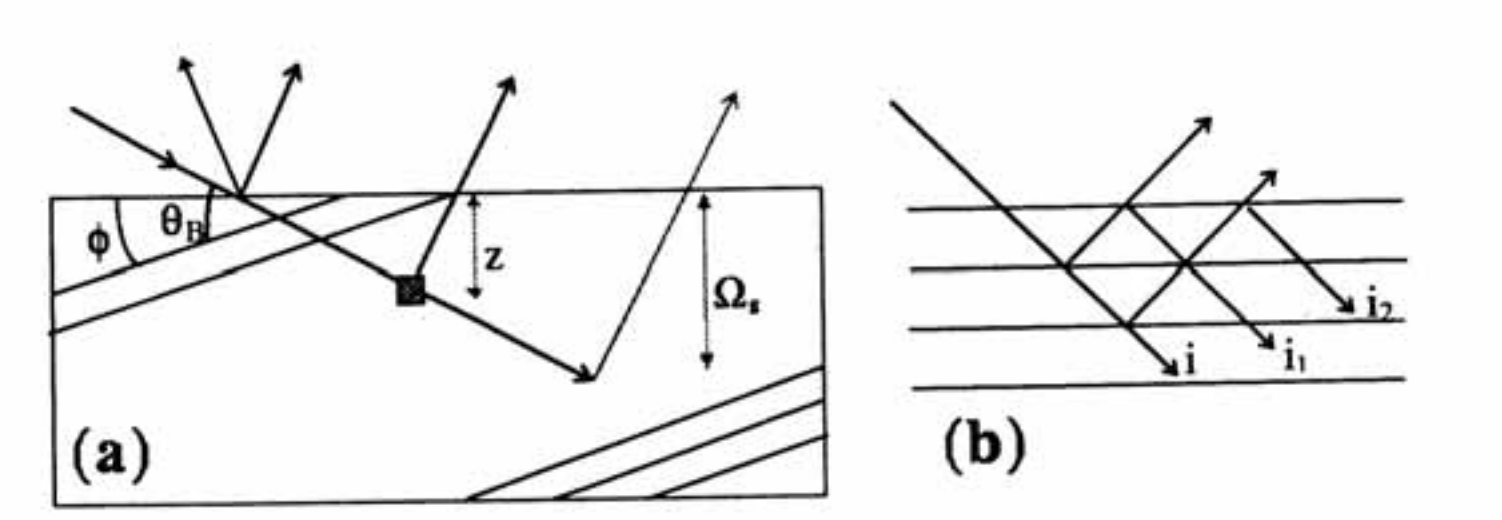

Penetration of x-rays in an imperfect crystal; Ω_S= penetration depth defined as the depth from where diffracted intensity is 10% of that from surface

X-ray topography (XRT) results

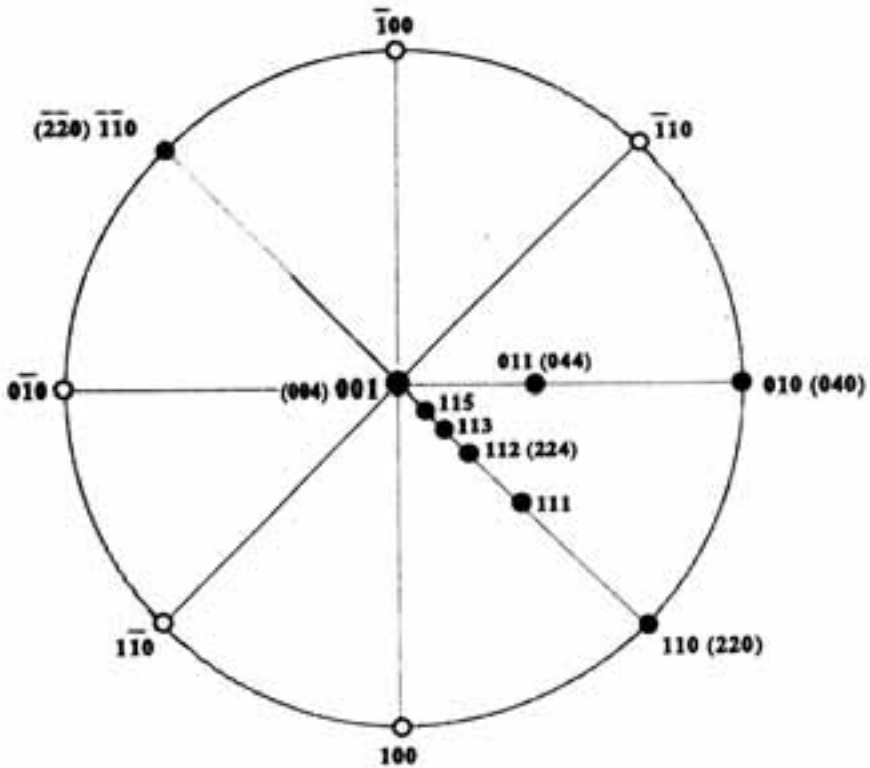

Sample	hkl	ϕ	θ_B	$\Delta\theta_A$	$\Delta\theta_R$	Ω_p	Ω_s	ρ_s/ρ_p
Si	113	25.3	28.1	12.9	0.8	0.8	7.6	2.5
	004	0	34.6	3.6	3.6	1.7	46.3	6.9
	224	35.3	44.0	7.6	1.2	1.3	21.5	4.2
	115	15.8	47.5	2.6	1.5	3.5	54.0	3.9
	044	45.0	53.4	7.4	1.1	1.4	20.7	3.7
GaAs	113	25.3	26.9	38.3	1.4	0.3	1.5	1.5
	004	0	33.0	8.2	8.2	0.7	15.5	5.4
	224	35.3	41.9	19.3	2.3	0.5	5.8	2.9
	115	15.8	45.1	6.0	3.3	1.5	17.9	3.1
	044	45.0	50.4	19.4	1.8	0.5	4.9	2.4

Sample	Radiation	hkl	ϕ	θ_B	$\Delta\theta$	ξ	μt
Si	Cu	111	54.8	14.2	8.3	15.0	7.1
		220	90	23.7	5.3	14.9	7.1
		022	45	23.7	8.5	9.5	7.1
		040	90	34.6	3.6	15.6	7.1
	Mo	111	54.8	6.5	3.4	33.6	0.7
		220	90	10.7	2.3	34.9	0.7
		040	90	15.2	1.4	40.0	0.7
		044	45	21.7	1.3	30.9	0.7
GaAs	Cu	111	54.8	13.6	18.5	13.1	20.2
		220	90	22.7	12.4	6.6	20.2
		022	45	22.7	19.4	4.3	20.2
		040	90	33.0	8.2	7.1	20.2
	Mo	111	54.8	6.2	8.1	14.7	17.3
		220	90	10.2	5.7	14.4	17.3
		040	90	14.6	3.5	16.5	17.3
		044	45	20.8	3.1	13.1	17.3

X-ray topography (XRT) results

In XRT, Bragg's diffraction rule $K_g = K + g$, is employed to scan a sample face to do topography. The intensity selection rule g.b decides the observed pattern, where b is a strain vector and g the reciprocal lattice vector.

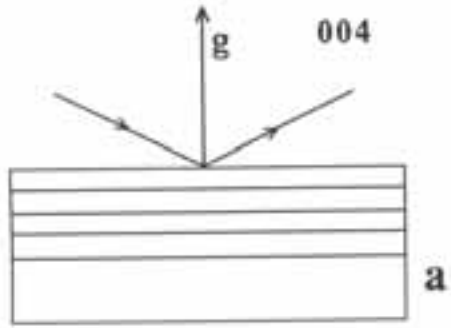

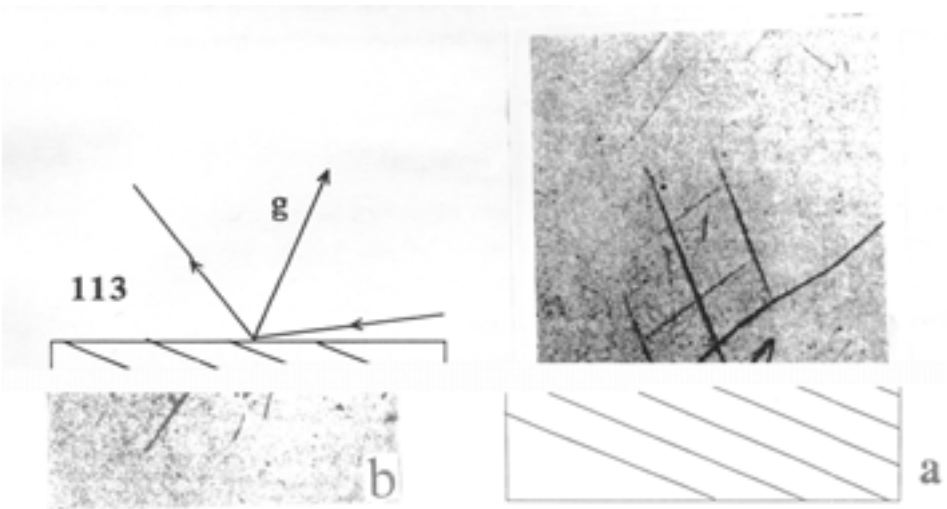

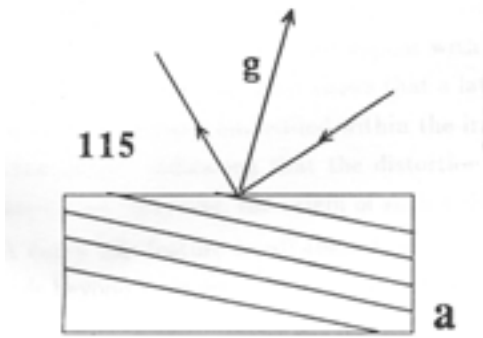

X-ray topography (XRT) results: Ti irradiation

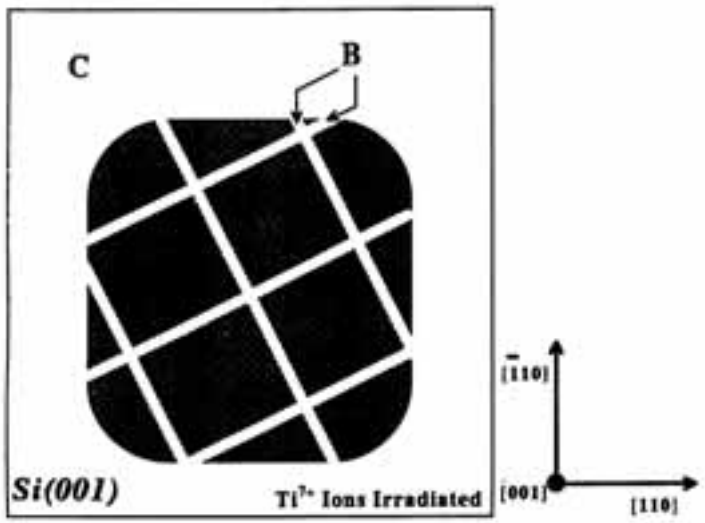

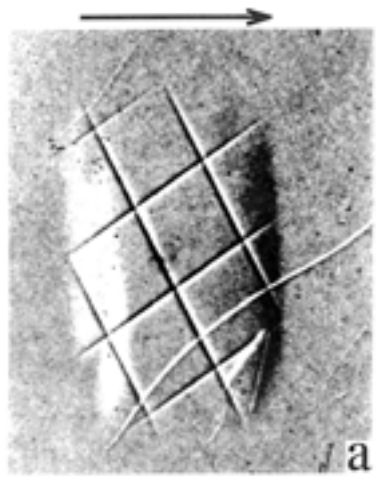

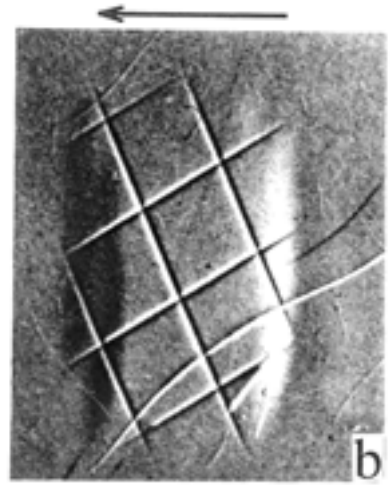

Grid held at approx. 30 degrees to [110] direction

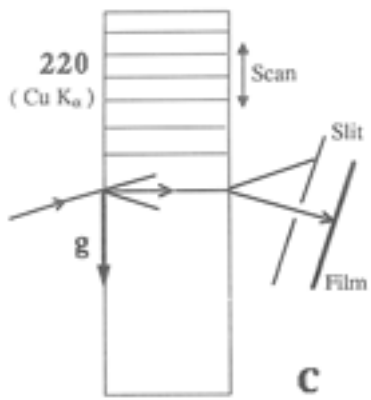

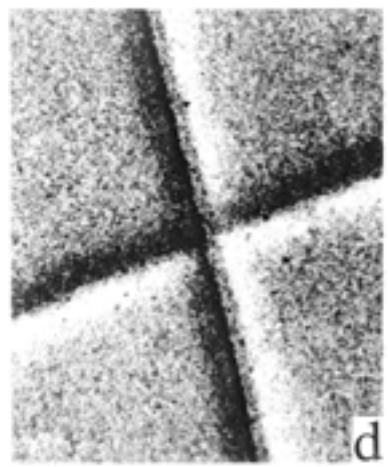

X-ray topography (XRT) results: Ti irradiation

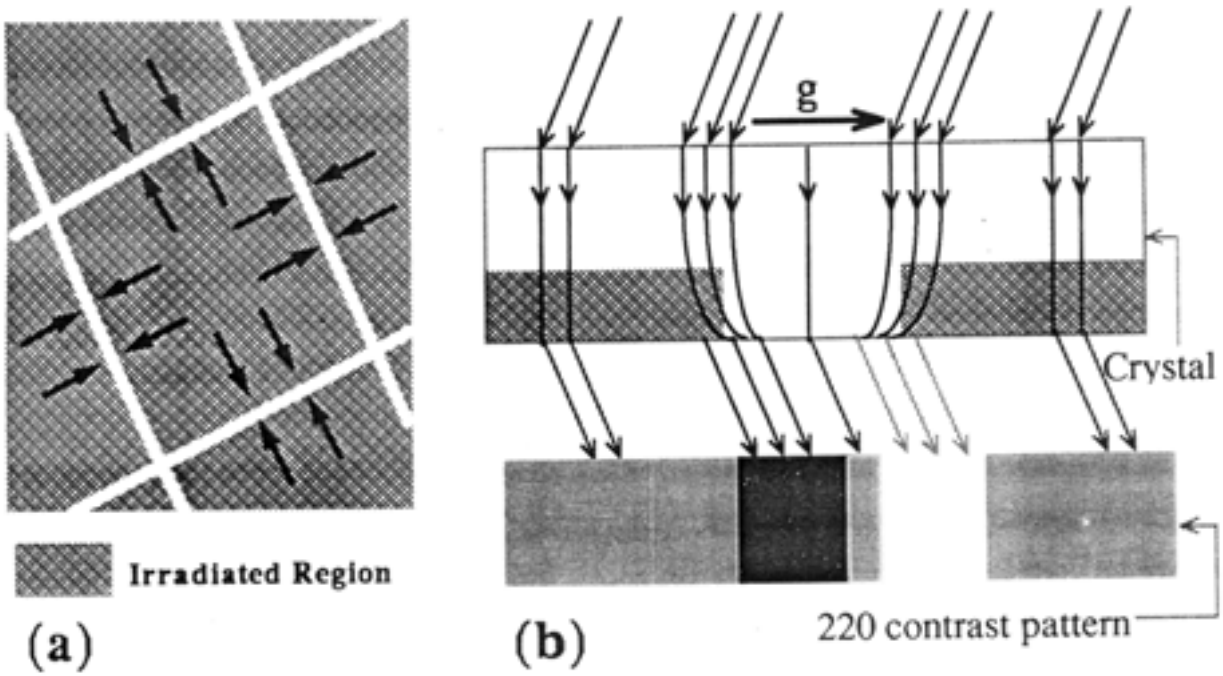

Origin of black – white contrast

X-ray topography (XRT) results: Ag irradiation

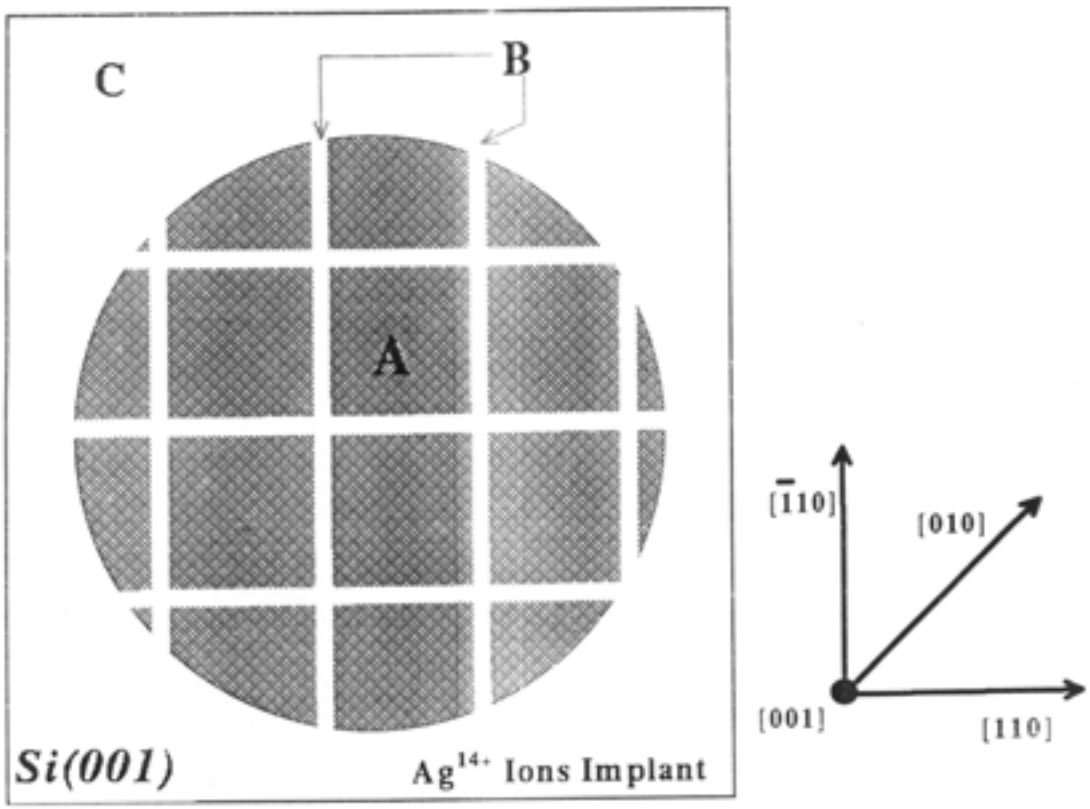

Geometry : One set of grids is held parallel to the [110] direction

X-ray topography (XRT) results

In XRT, Bragg's diffraction rule $K_g = K + g$, is employed to scan a sample face to do topography. The intensity selection rule g.b decides the observed pattern, where b is a strain vector and g the reciprocal lattice vector.

XRT picture of the 200 MeV Ag ion irradiated Si(100) face when g_{220} is in the direction as shown by arrow on top, employed to do XRT.

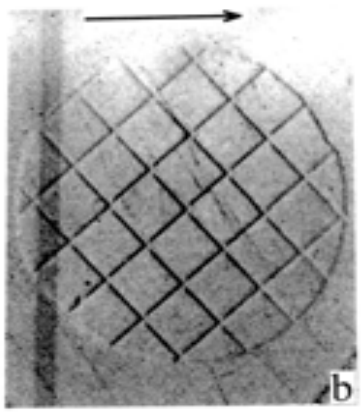

XRT picture of the 200 MeV Ag ion irradiated Si(100) face when the arrow on top is the direction of g_{040}, employed to do XRT.

Result:

Strain orientation is such that in XRT one set of lines are missing as g_{220} .b =0 for these while g_{040}.b is $\neq$ 0 for any strain generated. Also, the observed strain is perpendicular to beam direction and irradiation interface.

XRT result of stress distribution with depth inside MeV irradiated silicon

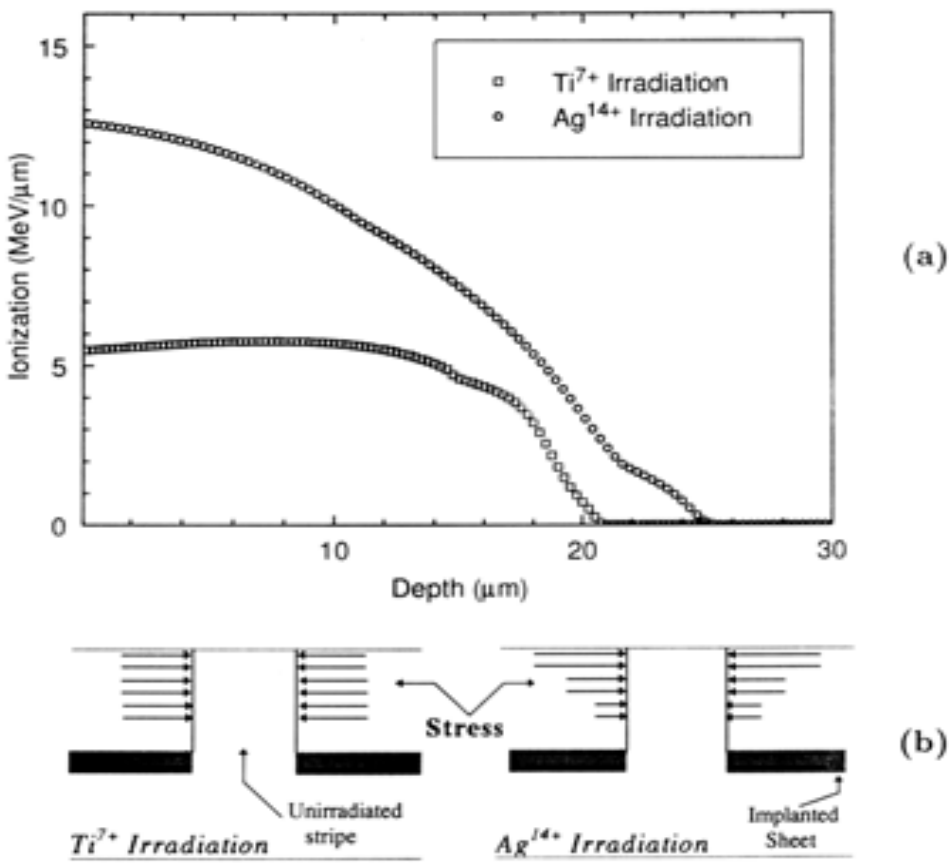

(a) **The electronic energy loss of 200 MeV Ag and 100 MeV Ti ions as shown before.**

(b) **The stress distribution inside the sample due to these two ions as revealed by XRT (line intensity profile). This was achieved by successive etching of the sample.**

Scanning Tunnelling Microscopy (STM) of the region under the Ni mesh

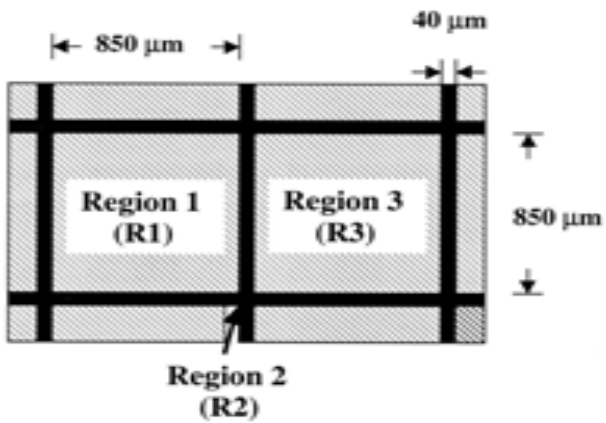

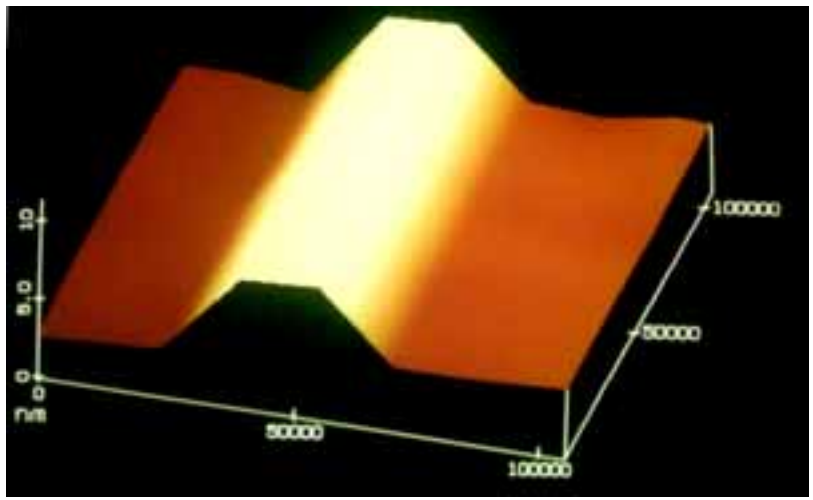

Region 1 = 200 MeV Ag ion irradiated; energy loss (dE/dx)e = 12.5 MeV/μm

Region 2 = region under the Ni wire (width = 40 μm)

Region 3 = 200 MeV Ag ion irradiated; energy loss $(dE/dx)_e$ = 12.5 MeV/μm

STM of the regions R1, R2 and R3. This can be viewed as an enlarged version of a single line as seen by XRT. R2 is raised. ***The raised portion in the figure is just below the wire mask. The ions do not reach here.*** **The plateau width = 15 μm.**

Irradiation Interface defects and their scaling with temperature

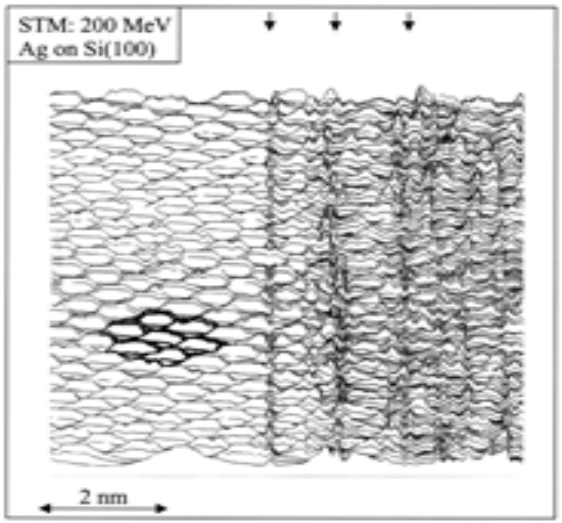

Details of the Irradiation Interface. The ions irradiate the sample on the left side which shows Si atoms with hexagonal symmetry which is the reconstructed Si c(2x1) structure. Sample as received.

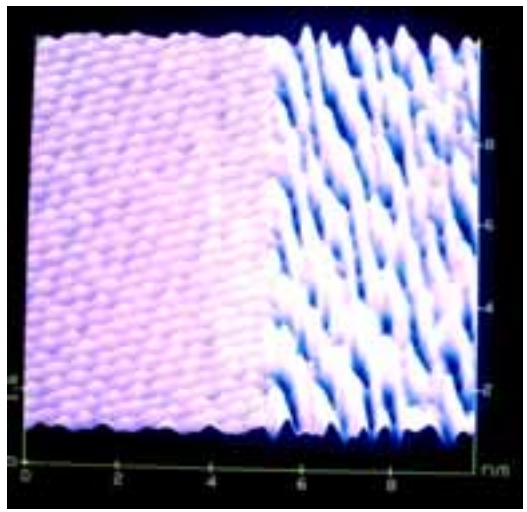

The as received sample after heating to 1150 K. All known point defects in Si disappear at this temperature. The artificial reordering at the Irradiation Interface are stable. The Si c(2x1) structure is retained.

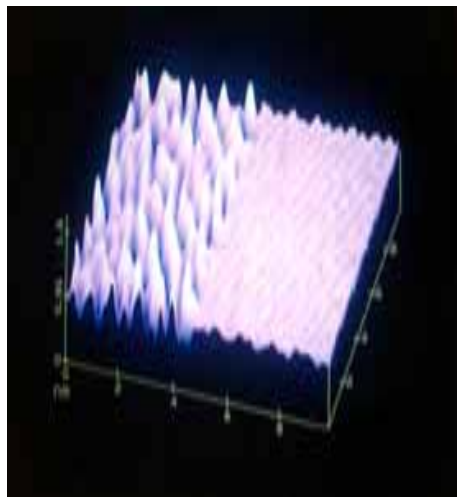

Another view of STM of Si(100). These are symmetrically placed on the other side of the impenetrable wire mesh.

Irradiation Interface defects and their scaling with the electronic energy loss, S_e

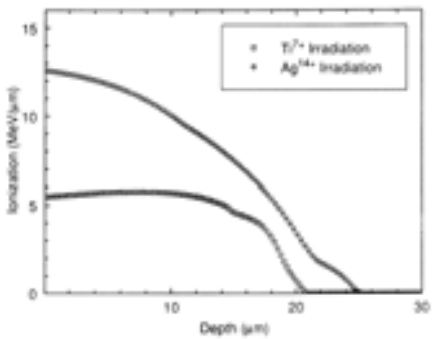

STM from a depth is achieved by carefully etching out layer by layer of Si atoms, chemically. Energy loss at a depth of 10 µm here is approx. 8 MeV/µm.

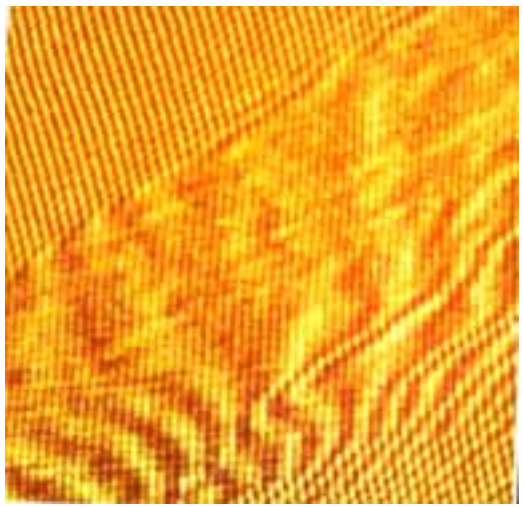

STM of Irradiation Interface from a depth of 10 µm . The energy loss $(dE/dx)_e$ = 8 MeV/µm. The irradiation front comes from the near corner. Interface width = 15 nm.

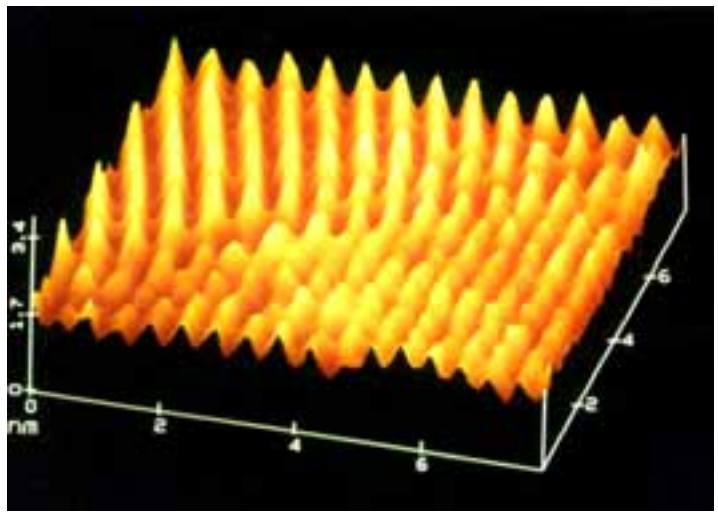

STM of the far corner of the picture on the left. This shows perfect periodicity next to a partially periodic lattice.

Further STM data from a depth of 10 μm

Inside Irradiation Interface

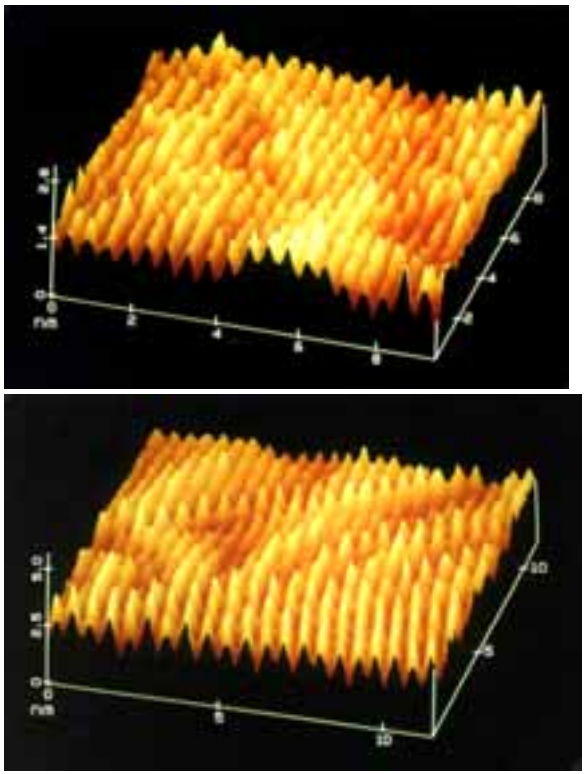

Si(100) surface from inside the Irradiation Interface. The ordering of atoms is lost in one direction. This can be easily seen by observing the edge of the 3-dimensional projection.

Reference regions

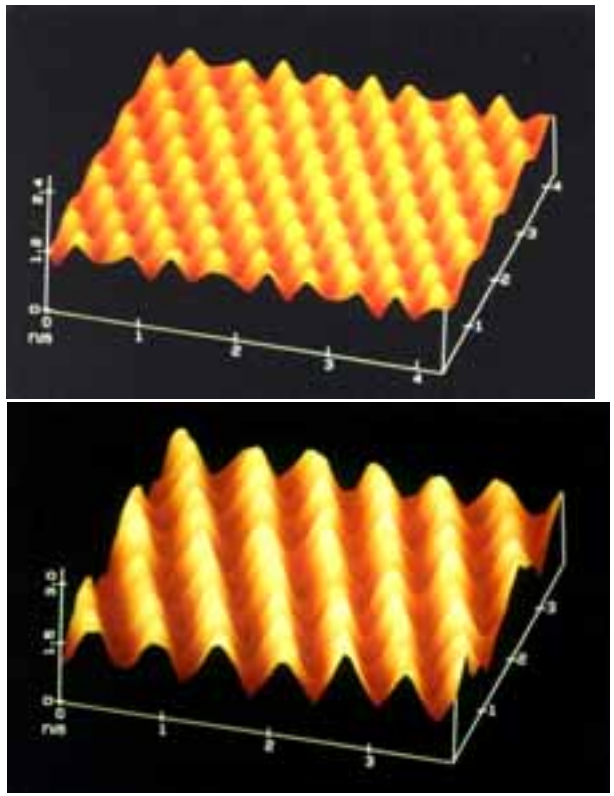

<u>Upper picture</u>: The reference Si(100) surface : a section left protected under a thick mask.
<u>Lower picture</u>: The Si(100) surface from the centre of irradiation, but towards the Irradiation Interface. Atomic Ordering is not lost.

The result so far

Observation of energy transport through the periodic Si lattice. Lattice acts as highways.

Observation of packets of atoms, representing differing energy content of the packets. The energy content of the packets scale with the energy loss suffered by the MeV ion.

Irradiation Interface length = 15 μm for S_e = 12 MeV/ μm.

Irradiation Interface length = 10 nm for S_e = 8 MeV/ μm.

Is there any other evidence for efficient energy transport ?

Yes.

K.H. Ecker and K.L. Merkle (Phys. Rev. B18, 1020,1978); and the famous **Wehner experiments (G.K. Wehner, J. Appl. Phys. 26, 1056, 1956 and G.K. Wehner, Phys. Rev. 102, 690, 1957) still remain unexplained .**

The Ecker – Merkle experiment: In support of R.H. Silsbee's idea of focusons

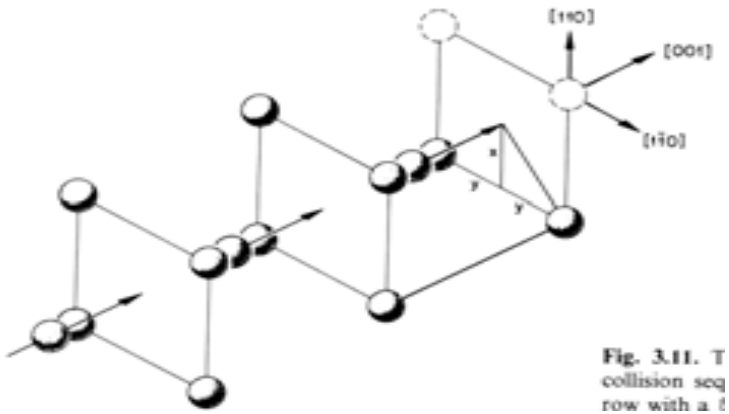

Fig. 3.11. T
collision seq
row with a

The idea of focusons is based on the assumption that energy gets focused in the forward direction, ejecting the terminal atom which exits from the other side in a transmission experiment. Focusons were thought to be defocussing when they did not work. (R.H. Silsbee, J. Appl. Phys. 28, 1246, 1957).

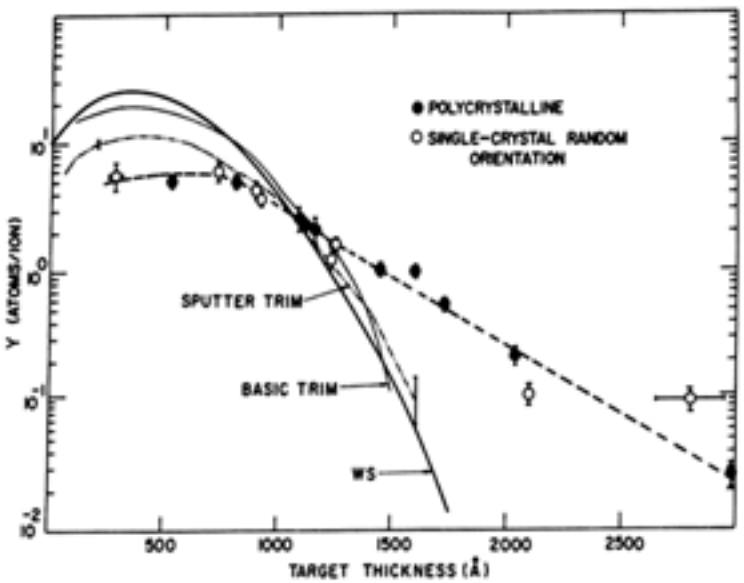

Ecker-Merkle experiment: 250 keV Ar ion impacted ejection of Au atoms from Au foils, in transmission. Au atoms were found in transmission even though the foil thickness were larger than range of the Ar ions.

The Wehner experiments

The Wehner observations on backscattering:

Observed as **backscattered target atoms** with **low, incident primary ion energy** such as **50 – 150 eV Hg ions**; first observed for a single crystal Ag target. The **calculated penetration depth is 0.1 nm.**

Backscattering is **not observed** for **long, evenly spaced chains of atoms**. They have been **observed from the (111) direction of crystals** with **the diamond or zinc-blende structures**.

The atom sequences along various directions are :

100 = atom atom atom atom with atom –atom separation = a (focuson OK)

110 = atom atom atom atom with atom –atom separation = 0.707a (focuson OK)

111 = atom atom blank blank atom etc. with atom-atom or blank-blank separation = 0.25a (focuson not OK). Atoms are backscattered in this direction.

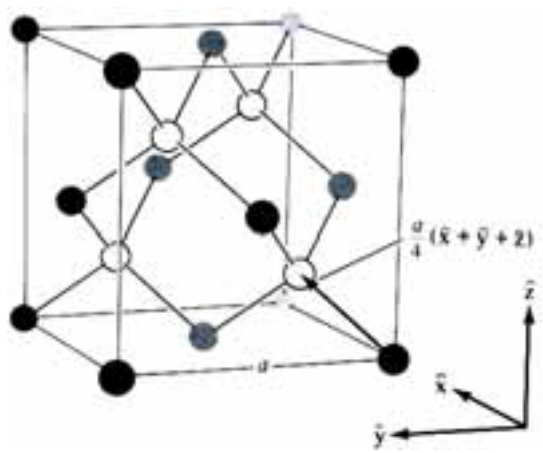

What prompted the top layer atoms, in a lattice with diamond structure, to backscatter preferentially in the (111) direction ?

As there was no forward momentum transfer, energy required to overcome the cohesive energy was obtained from the incident primary ion and stored as vibrational energy.

Is there a possibility for energy localisation?

Yes, in Lattice Solitons or Intrinsic Localised Modes.

Description of Lattice Solitons :

Solitons in continuous media arise due a balance between nonlinearity and dispersion. Energy is localised as seen in water waves.

In a solid, nonlinearity and lattice discreteness provides for localisation of energy. As nonlinearity is an intrinsic requirement according to its proponents (S.A. Kiselev, S.R. Bickham and A.J. Sievers, Comm. Cond. Matter Phys. 17, 135, 1995), these are Intrinsic localised modes (ILM).

In the presence of anharmonicity, new breather like modes get active in the gap between the acoustic and optic branches.

Our evidence for energy localisation

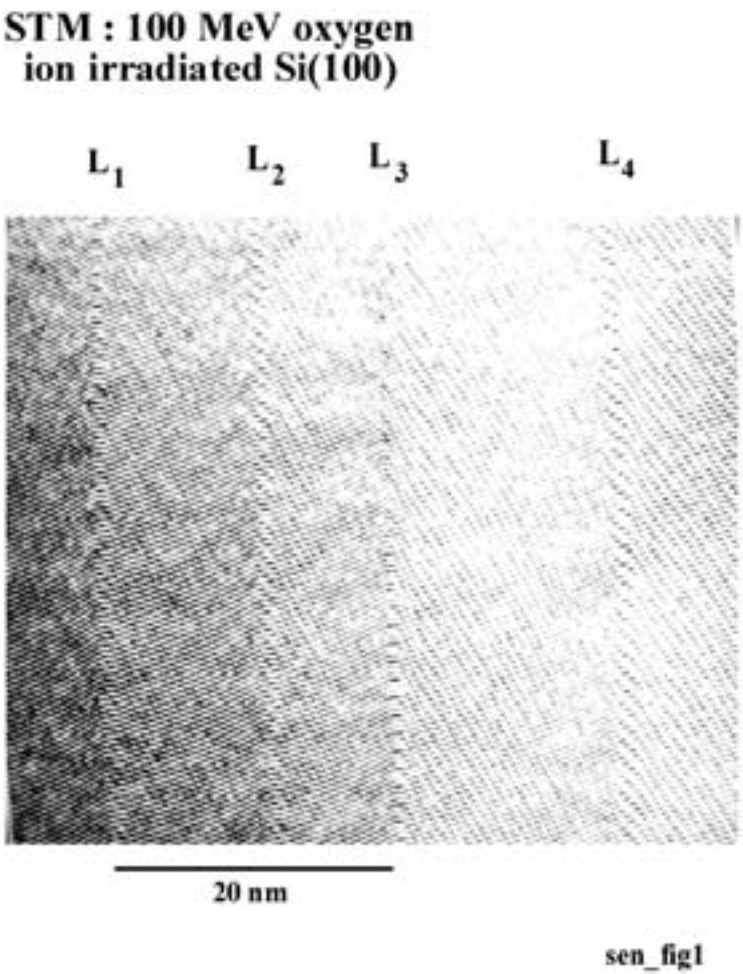

100 MeV oxygen on Si(100)

A 50 nm x 50 nm STM scan of the 100 MeV oxygen ion irradiated Si(100) face is shown. The oxygen ions enter the Si lattice normal to the (100) face. The STM image is marked by four vertical columns of atoms (marked L_1, L_2, L_3 and L_4 from left) whose interatomic distances are distinct from the periodic lattice present in their immediate surrounding. These are disturbances, whose origins lie at ion impact event that has taken place 500 nm away to the right.

STM of 100 MeV oxygen ion irradiated Si(100) : line L_2

100 MeV oxygen on Si(100)

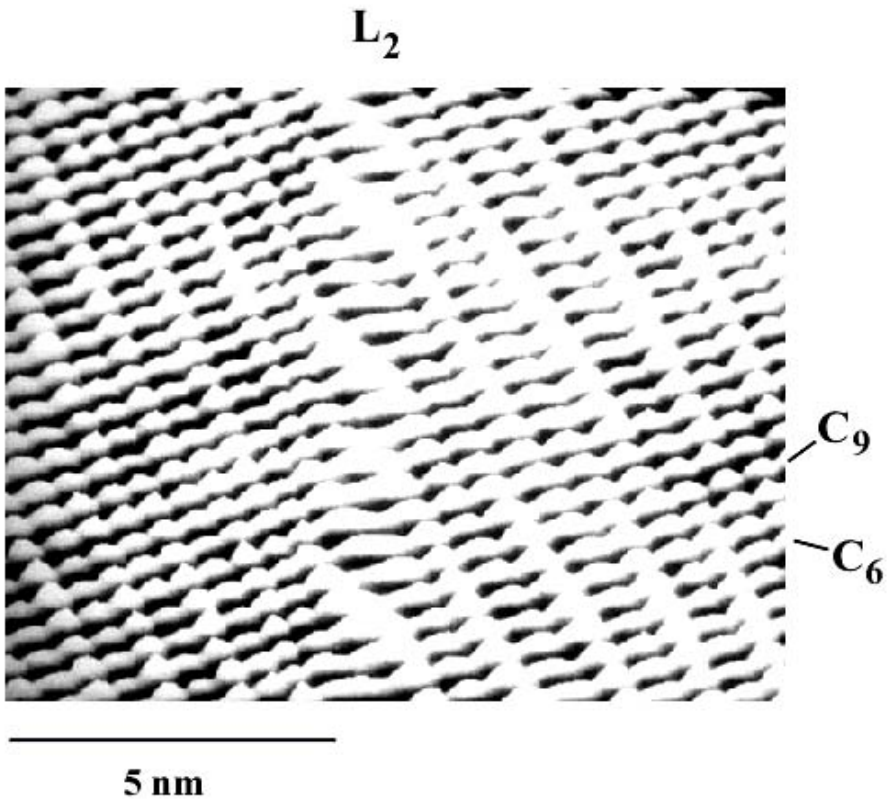

An expanded STM scan of the region marked L_2 of the last figure is shown here to expose details of the vertical column of atoms. The column of disturbed atoms is placed 5 nm from the left edge of the figure and is prompted by an inherent lack of lattice periodicity spread over 3-4 atomic distances. The rest of the lattice, on either side of the 5-nm mark, remains periodic.

100 MeV oxygen on Si(100)

STM of 100 MeV oxygen ion irradiated Si(100) : line L_3

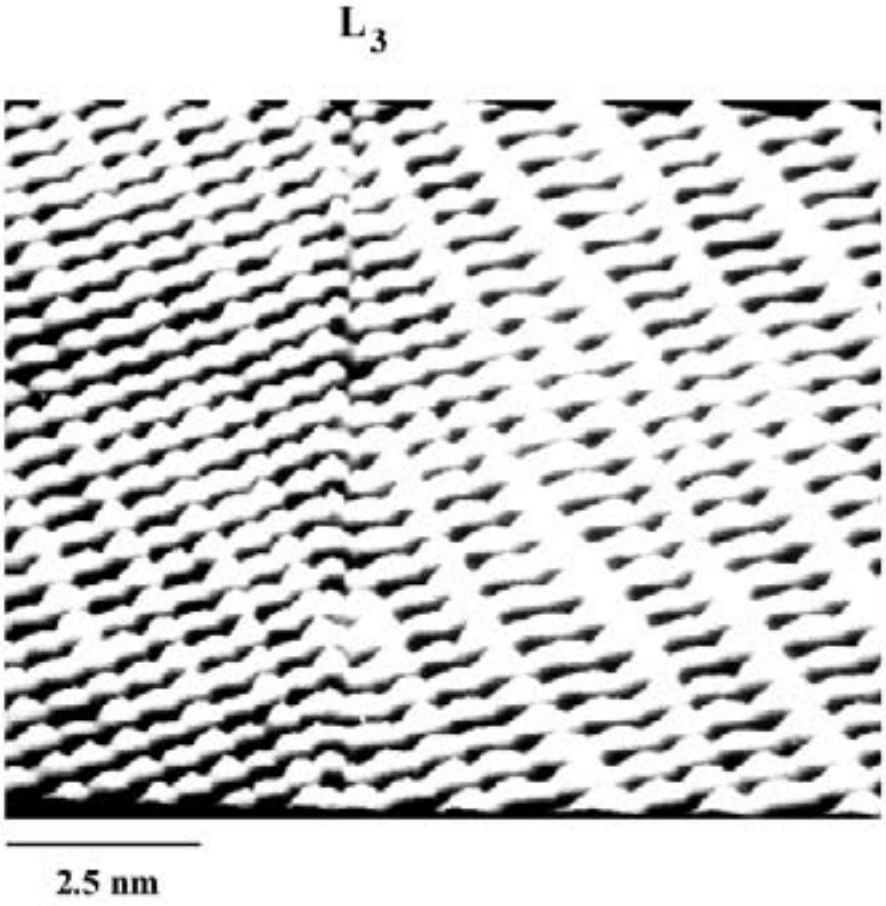

An expanded STM scan of the region marked L_3 of the earlier figure is shown here to show the loss in lattice periodicity in the upper section of L_3. The discontinuity is akin to crack formation and arises as the lattice strain developed in this region is released.

Measuring some properties

Irradiation Interfaces as Artificially Reordered structures ?

By <u>artificial</u> we mean that some properties of the original lattice has been modified artificially.

We use the method of scanning tunnelling spectroscopy to show the changes in electronic properties across the Irradiation Interfaces where the artificial reordering takes place.

In our experiment, we employ this technique to determine just the band gap. This is shown below.

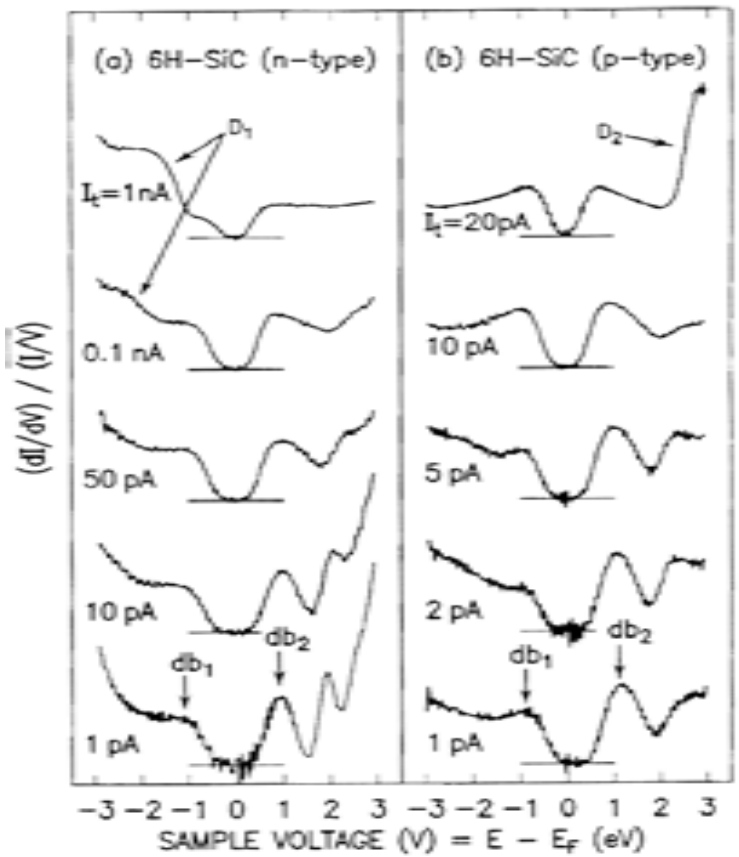

Ramachandran and Feenstra, (Phys. Rev. Letters, 82, 1000, 1999)

Bangap # 1

Band gap = 1.14 eV

Part of the 200 MeV Ag ion irradiated lattice. Lattice periodicity retained.

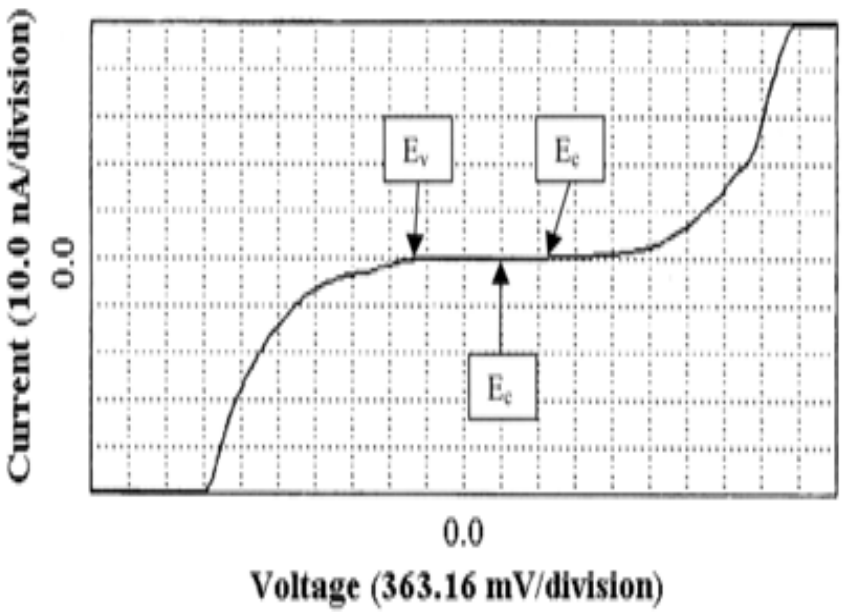

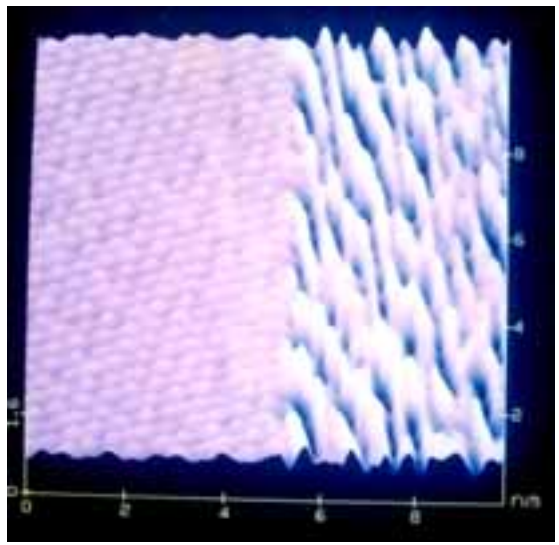

Bandgap # 2

Band gap = 0.4 eV

Part of the lattice not irradiated by 200 MeV Ag ions. Nanometer sized clusters of Si observed.

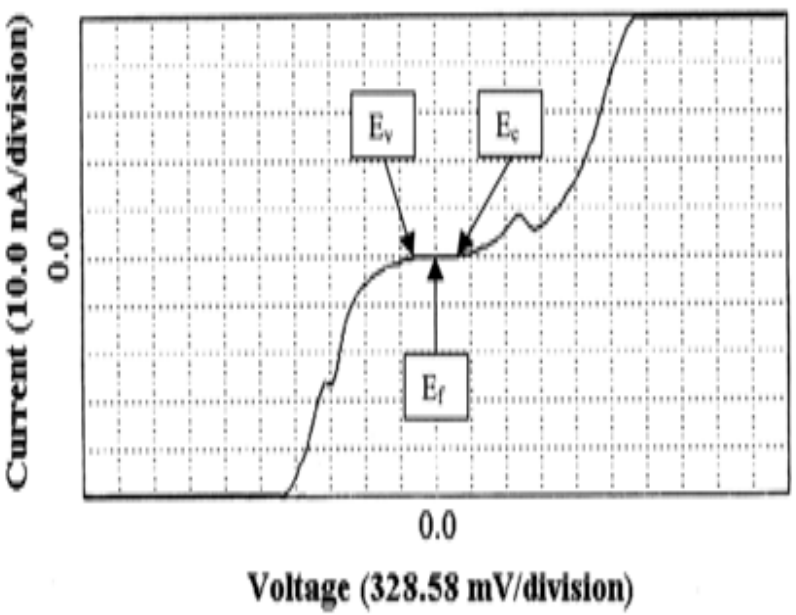

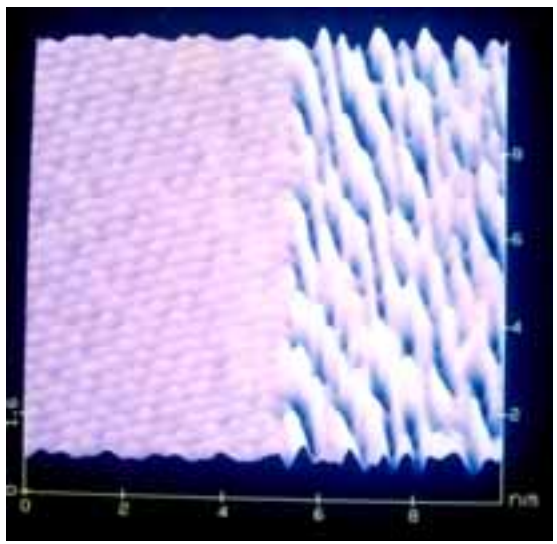

Bandgap # 3

Band gap = 2.1 eV

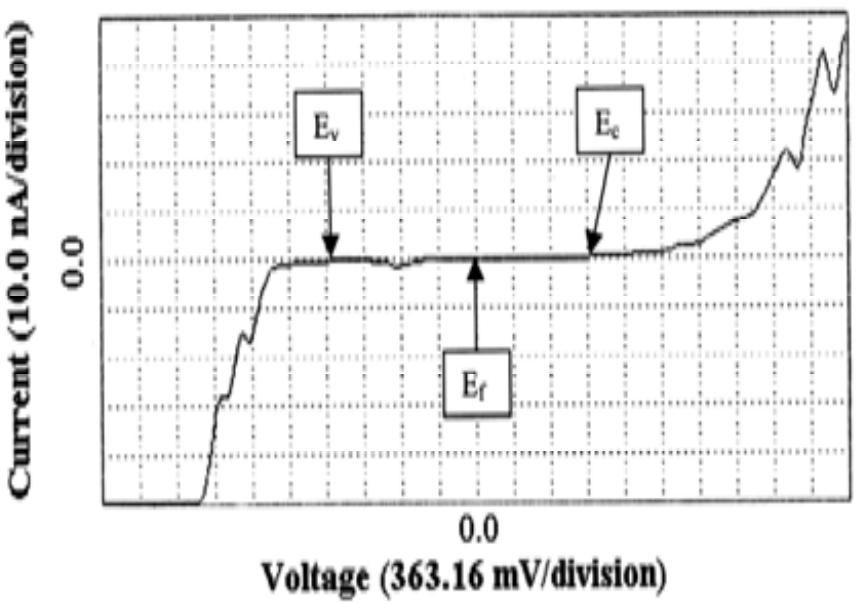

Oxidized Si(100) surface

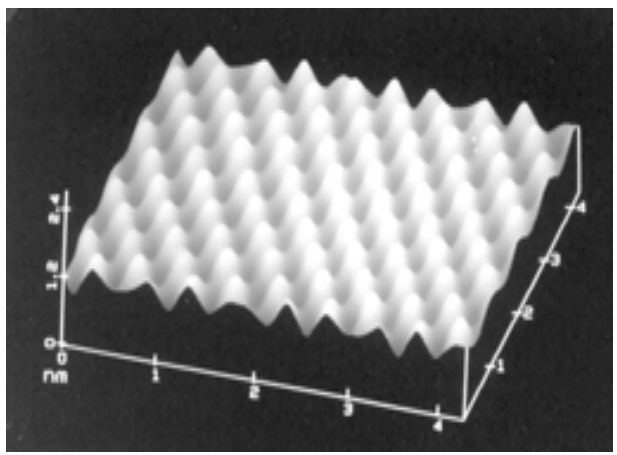

Silicon – The elixir of modern living

Silicon – the disadvantage

- Does not emit light
- Electronic signals cannot be transferred to optical pulses

Reason

- Indirect band gap
- Physically, an electron and hole recombination is made ineffective

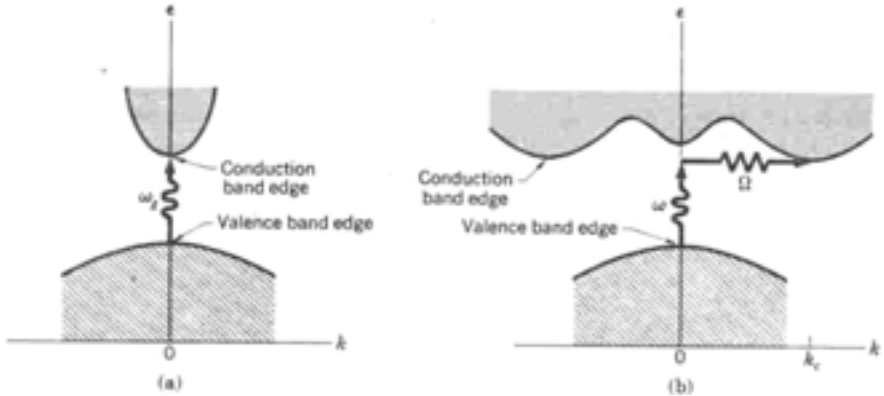

Indirect band gap in silicon. Energy absorbed is lost to the lattice.

On the left, the lowest point of the conduction band occurs at the same value of *k* as the highest point of the valence band (direct band gap). On the right, the band edges are widely separated in *k* space (hence indirect), involving both a phonon and a photon in the transition.

Is porous silicon the answer ?

A porous silicon sample illuminated by an Argon laser (Nature, Nov. 2000).

Light emission from silicon by L. Pavesi *et al.*, Nature Nov. 2000

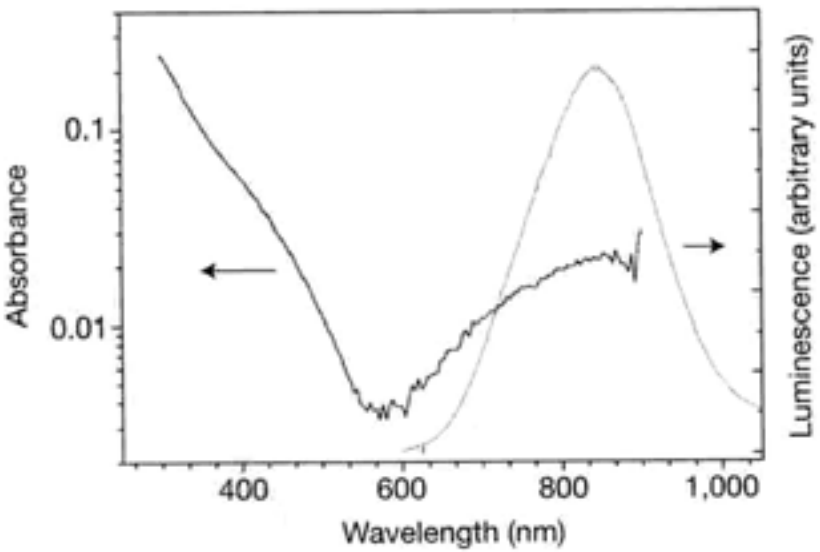

Room temperature absorbance and luminescence of Si nanocrystals embedded in quartz. Luminescence was excited with an Argon laser (488nm).

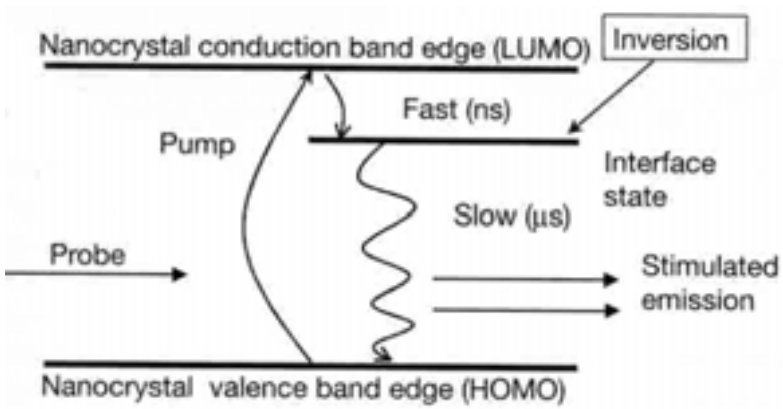

Schematic energy diagram for a nanocrystal showing how population inversion can be reached.

Light emission from silicon- a concept, compatible with existing silicon devices

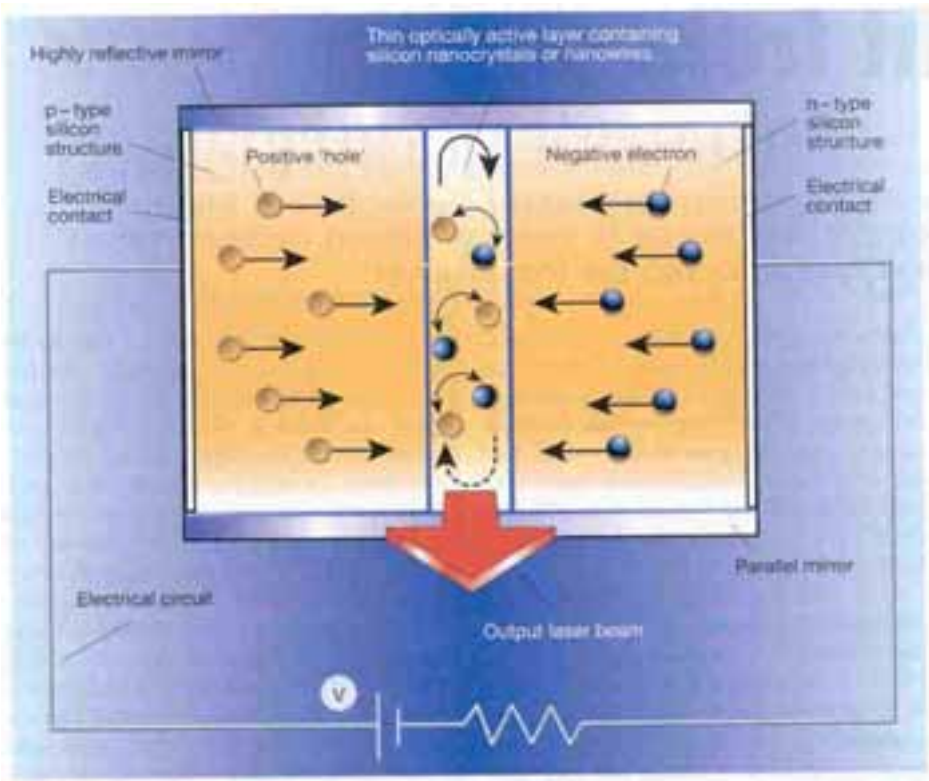

How an electrically driven silicon light emitter might work in the future.

Electrically driven emission of light from semiconductors is the basis for light emitting diodes through recombination of an electron and hole inside the semiconductor. The challenge in silicon is to have nanocrystals compacted between p- and n-type silicon, electrically drive the electrons and holes into the nanocrystals to achieve light emission.

The desired configuration

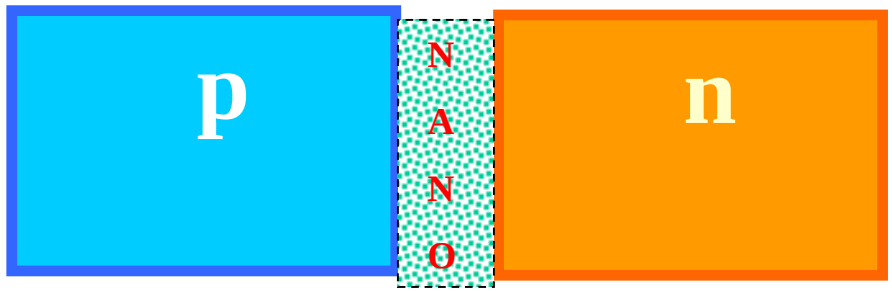

Requirements:

(1) The p-side as well as the n-side have to be doped single crystalline lattices.

(2) Nanostructures have to be placed intermediate these regions and contiguous with the single crystalline material. Purity is essential.

(3) The entire combination should be of sufficient thickness.

(4) Should be compatible with device fabrication techniques.

Present Status : None compatible

Our suggestion : Nonlinear energy transport

The nanostructured p-n junction

Achievements of MeV ion induced Artificial Reordering of Si

Nanostructures can be placed contiguous to a single crystalline lattice of silicon.

Interfaces between crystalline-nano are extremely sharp.

The entire combination is (at least in this case) 24 µm thick.

Is it compatible with standard device fabrication process ?

Next : A nanostructured p-n junction fabrication

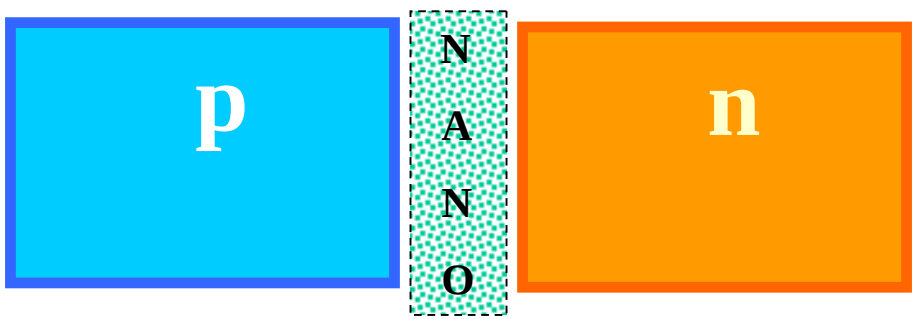

The nanostructured p-n junction device fabrication

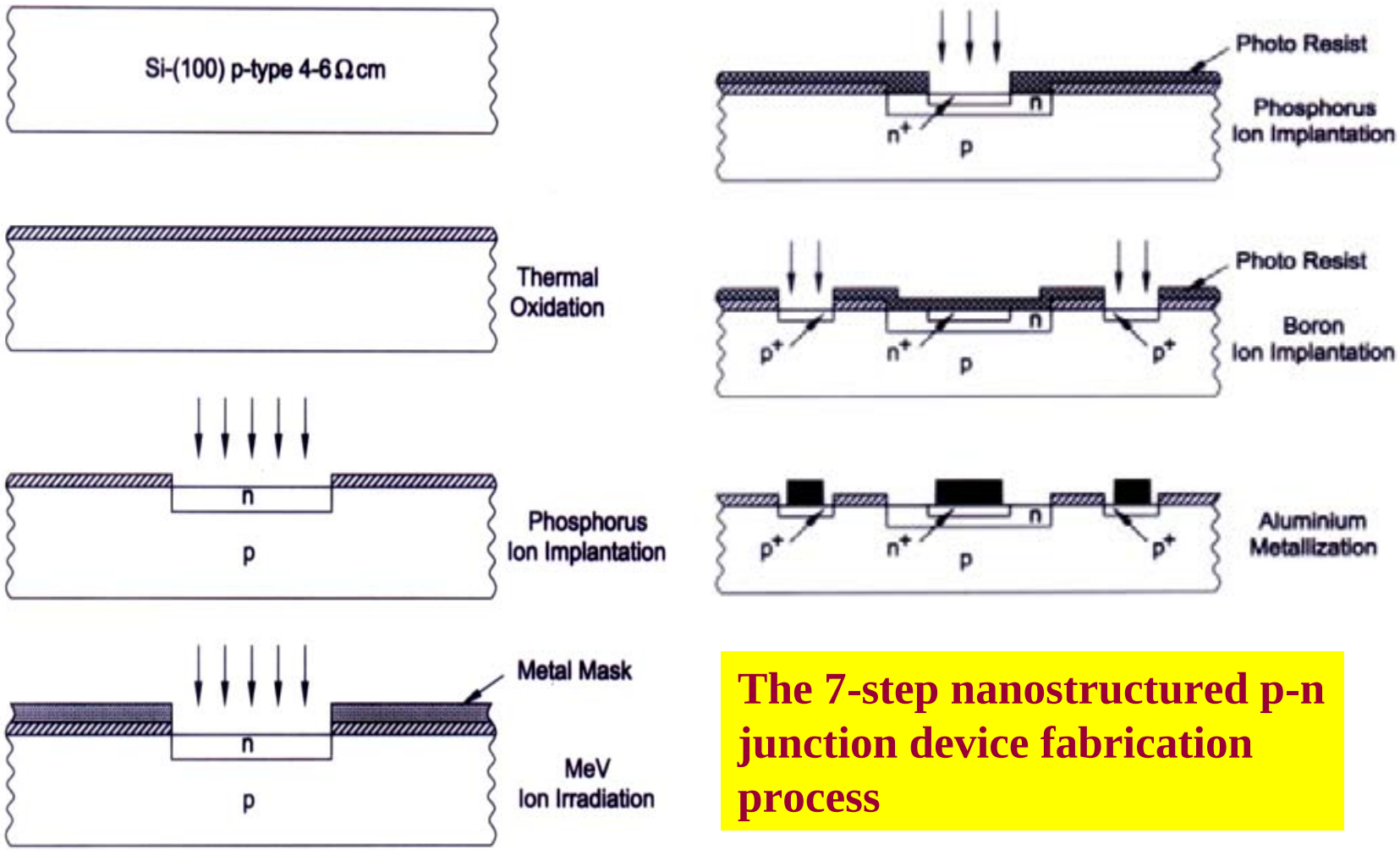

The 7-step nanostructured p-n junction device fabrication process

Do we get light from the nano- sandwitched p-n junction device ?

Not yet. Some indicators.

Problem: Fine tuning of the nanostructured Si.

Biasing the junction provides interesting insight.

Biasing the nanostructured p-n junction

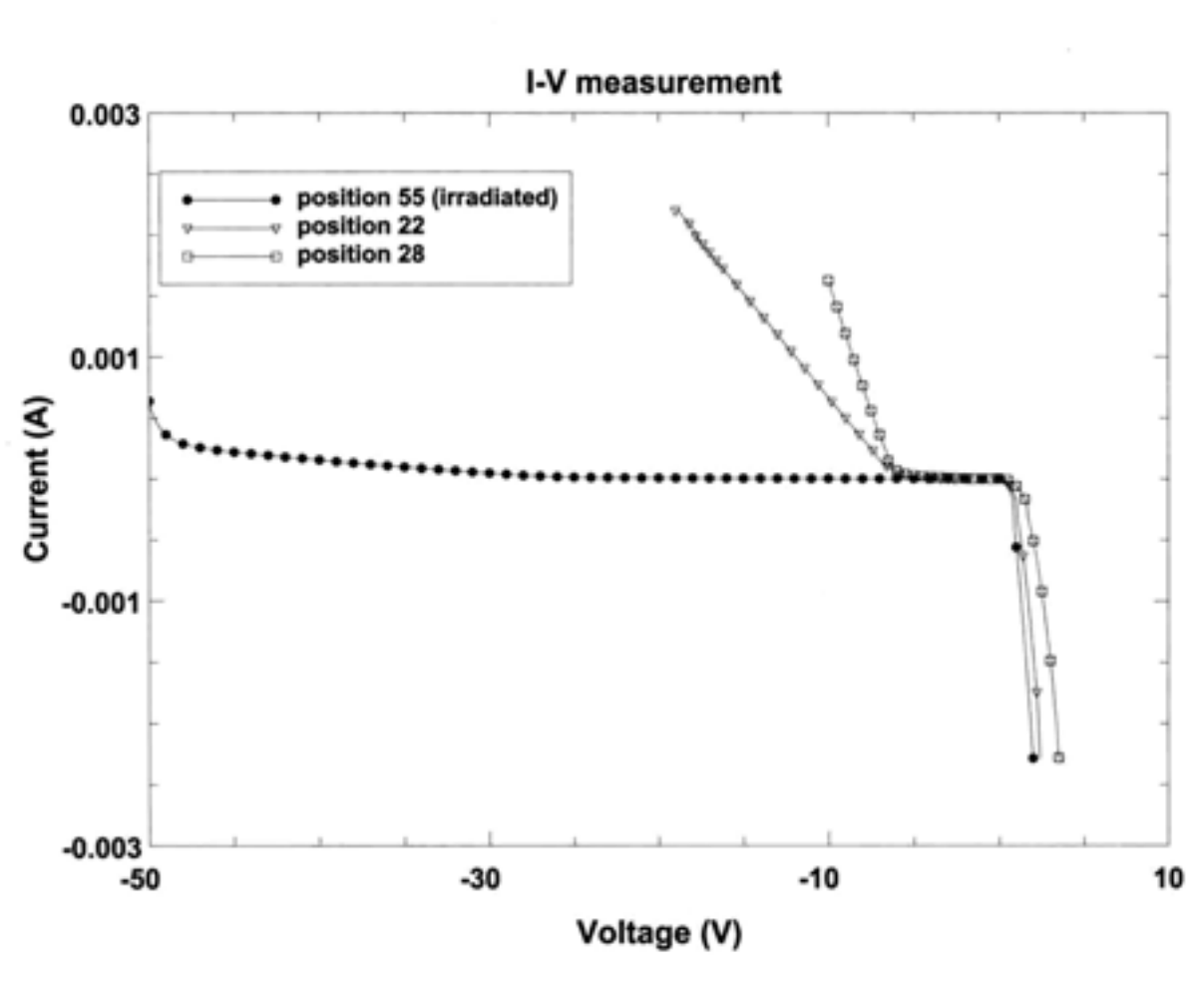

The reverse biased nanostructured p-n junction shows marked improvement in breakdown voltage (from 6V → 48V) and leakage current.

Forward biasing behaviour remains unaltered.

Biasing the nanostructured p-n junction (near V=0)

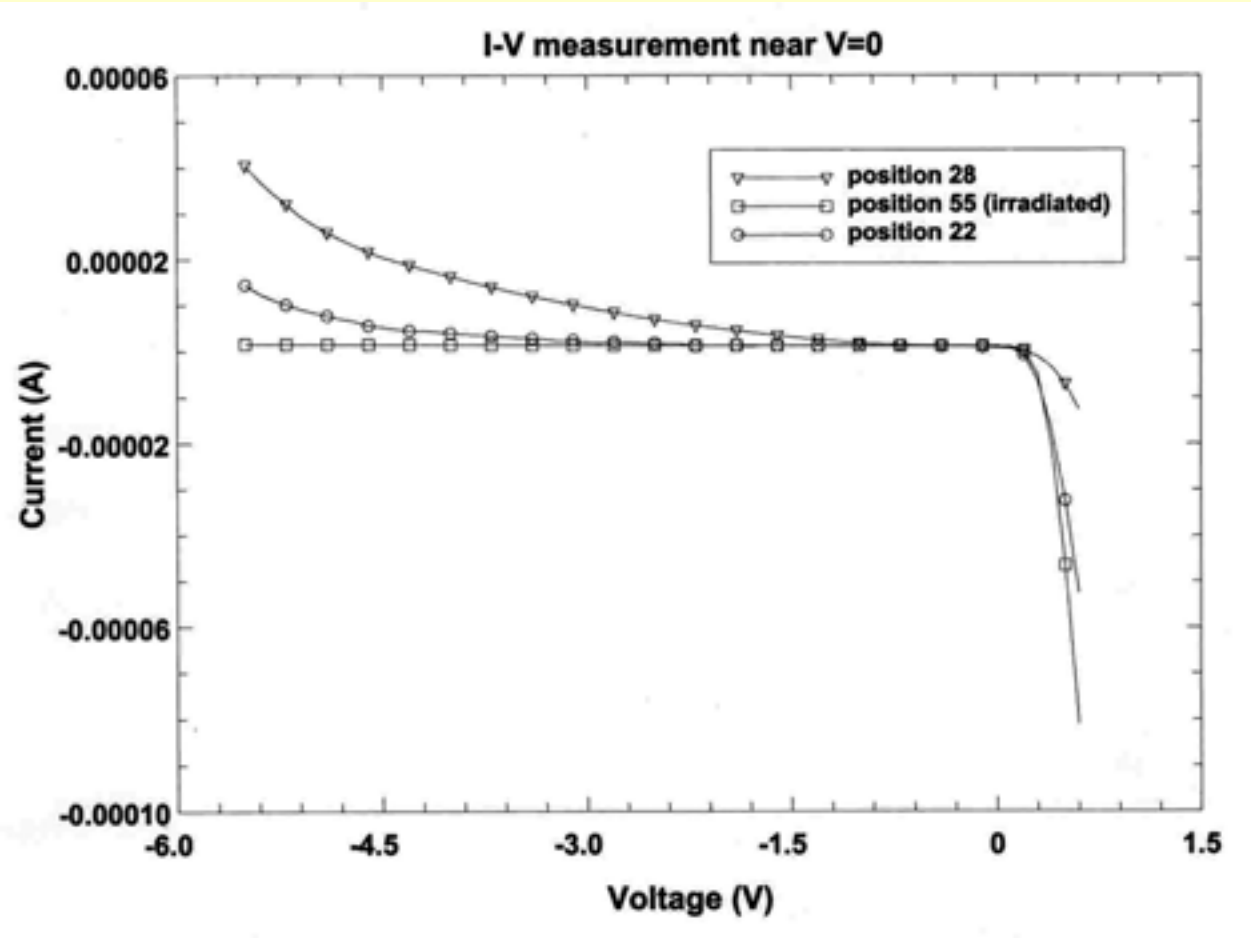

The reverse biased nanostructured p-n junction near V=0 showing reverse saturation current of 1 x 10^{-7} A (limited only by the capability of the measuring device) at V= – 6V as compared to a traditional p-n junction device with a reverse saturation current of 1 x 10^{-6} A.

Other results : Water adsorption on artificial structures of silicon

All snaps taken after an interval of 1 min from “a”

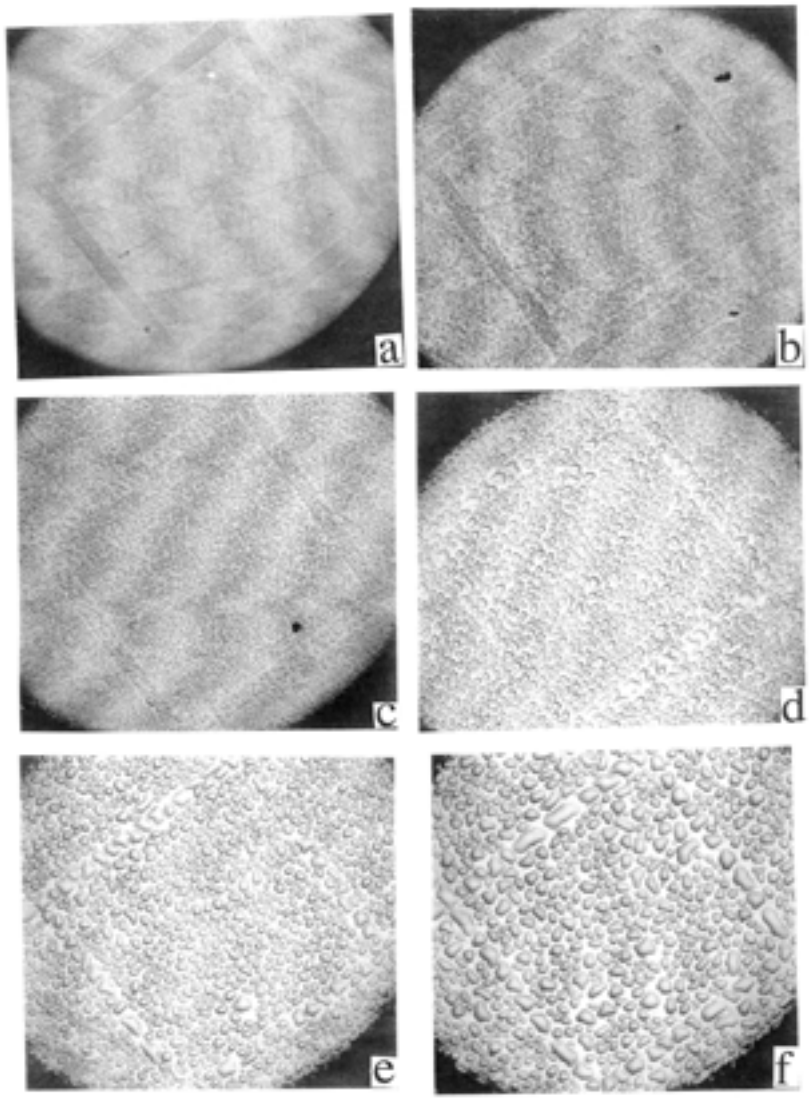

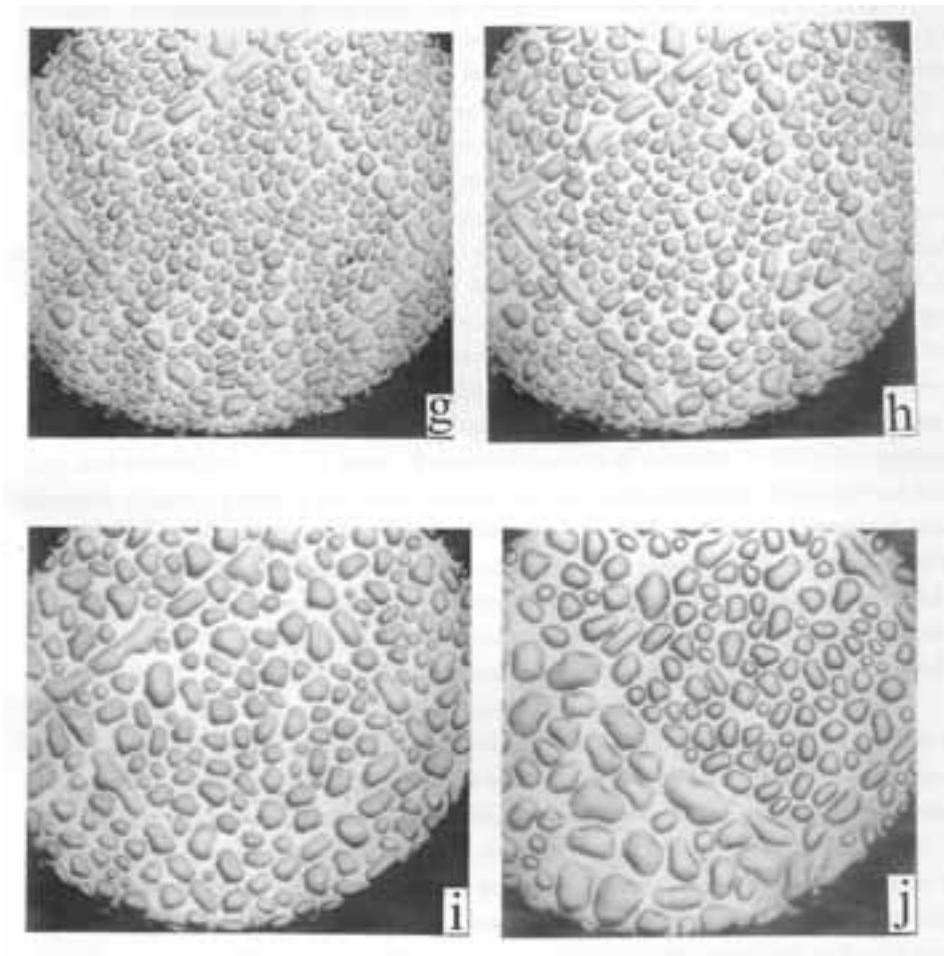

Other results : Water adsorption on artificial structures of GaAs

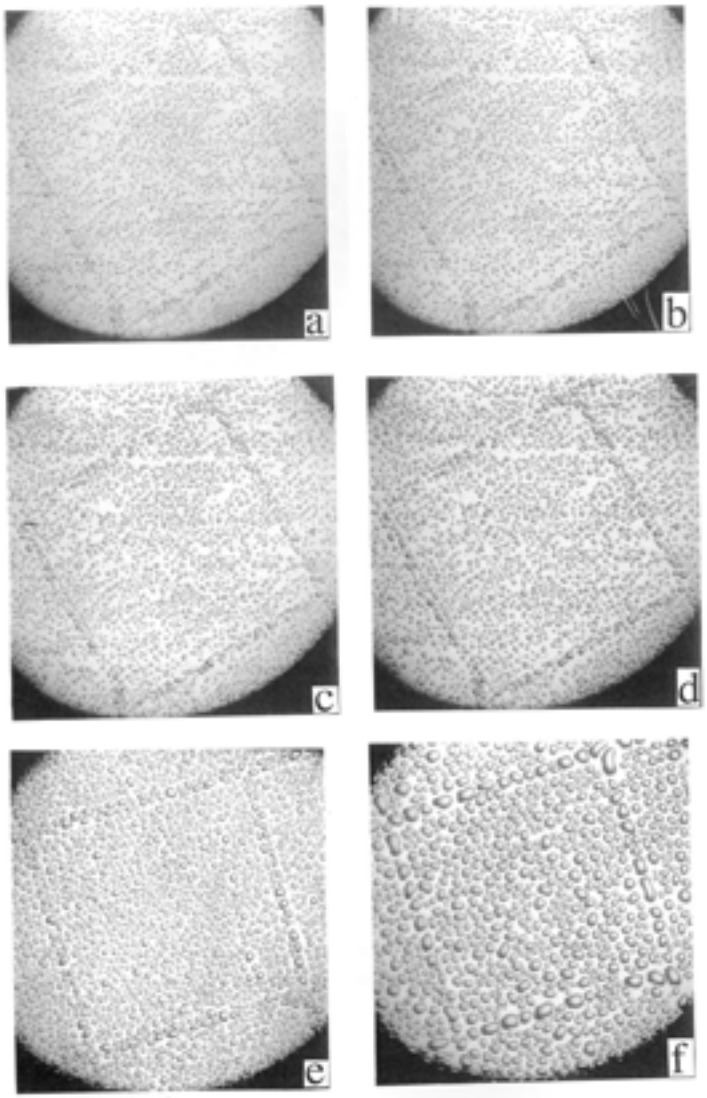

All snaps taken after an interval of 1 min from “a”

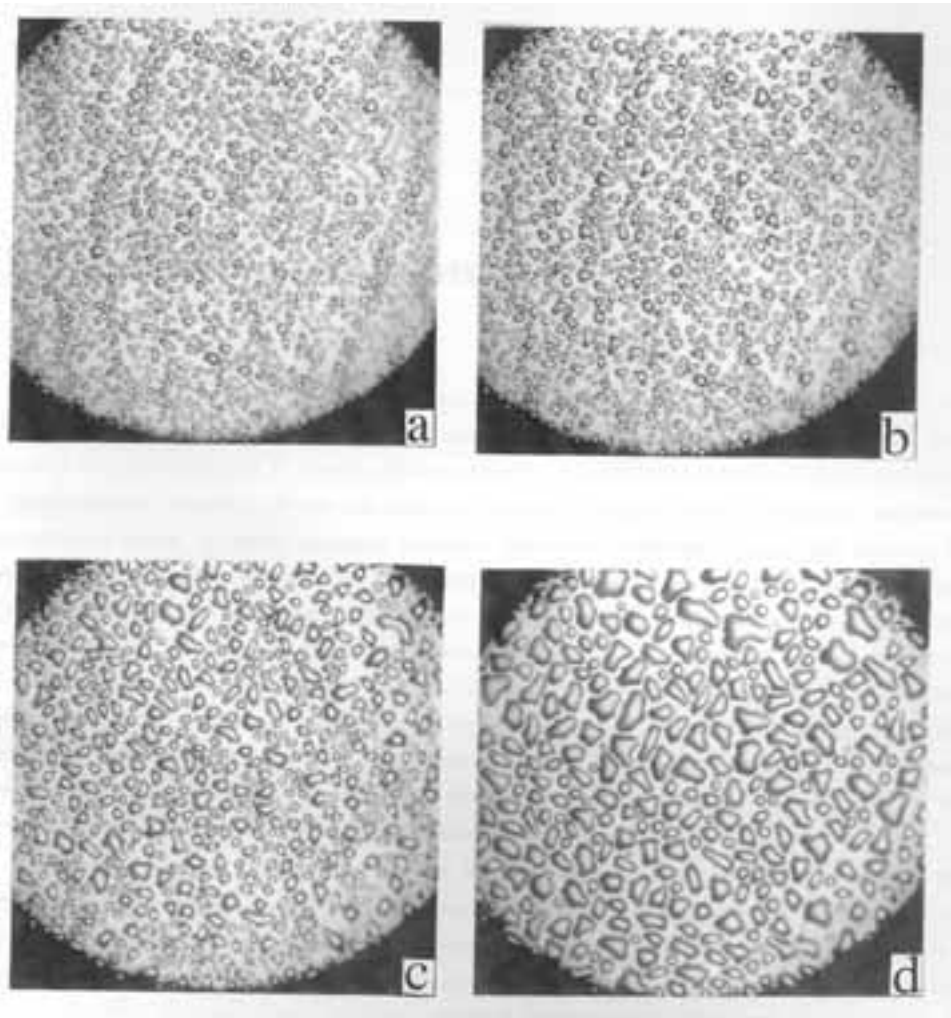

Conclusions

1. Shown that MeV ion irradiation can be suitably employed for producing artificial reordering of a single crystalline material like Si. Nonlinear transport of vibrational energy is the process employed.

2. A simple Si-based p-n junction device has been demonstrated to have exceptional breakdown property and leakage current behaviour in presence of nanostructured silicon.

3. Wehner experiment can possibly be understood after almost 50 years !!!

4. Proposals to remove defects are already in place by sweeping them away (under the carpet).

Acknowledgements

Jamil Akhtar

Gautam Aggarwal

Umesh Tiwari

Nuclear Science Centre for irradiation experiments

Publications etc.

This presentation, in part, came from:

1. P. Sen, G. Aggarwal and U. Tiwari, *Physical Review Letters*, Vol. 80, p. 97 (1998)

2. G. Aggarwal and P. Sen, *Europhysics Letters*, Vol. 44, p. 471 (1998)

3. P. Sen, J. Akhtar and F.M. Russell, *Europhysics Letters*, Vol. 51, p. 401 (2000)

4. P. Sen and J. Akhtar in "*Microcrystalline and Nanocrystalline Semiconductors*" MRS Symposium Proceedings Vol 638 (Pittsburg, 2001), Eds. J.M. Buriak *et al.*

4. P. Sen and J. Akhtar in Current Science Vol. 85, p. 1723 (2003)